

# Exploring the use of compound-specific carbon isotopes as a palaeoproductivity proxy off the coast of Adélie Land, East Antarctica

Kate Ashley<sup>1</sup>, Xavier Crosta<sup>2</sup>, Johan Etourneau<sup>2,3</sup>, Philippine Campagne<sup>2,4</sup>, Harry Gilchrist<sup>1</sup>, Uthmaan Ibraheem<sup>1</sup>, Sarah Greene<sup>1</sup>, Sabine Schmidt<sup>2</sup>, Yvette Eley<sup>1</sup>, Guillaume Massé<sup>4,5</sup> and James Bendle<sup>1</sup>

<sup>1</sup>School of Geography, Earth and Environmental Sciences, University of Birmingham, Edgbaston, Birmingham, B15 2TT, UK

<sup>2</sup>EPOC, UMR-CNRS 5805, Université de Bordeaux, 33615 Pessac, France

<sup>3</sup>EPHE/PSL Research University, 75014 Paris, France

<sup>4</sup>LOCEAN, UMR CNRS/UPCM/IRD/MNHN 7159, Université Pierre et Marie Curie, 4 Place Jussieu, 75252 Paris, France

<sup>5</sup>TAKUVIK, UMI 3376 UL/CNRS, Université Laval, 1045 avenue de la Médecine, Quebec City, Quebec, Canada G1V 0A6

*Correspondence to:* James Bendle (j.bendle@bham.ac.uk)

## Abstract

The Antarctic coastal zone is an area of high primary productivity, particularly within coastal polynyas where large phytoplankton blooms and drawdown of CO<sub>2</sub> occur. Reconstruction of historical primary productivity changes, and the associated driving factors, could provide baseline insights on the role of these areas as sinks for atmospheric CO<sub>2</sub>, especially in the context of projected changes in coastal Antarctic sea ice. Here we investigate the potential for using carbon isotopes ( $\delta^{13}\text{C}$ ) of fatty acids in marine sediments as a proxy for primary productivity. We use a highly resolved sediment core from off the coast of Adélie Land spanning the last ~400 years and monitor changes in the concentrations and  $\delta^{13}\text{C}$  of fatty acids along with other proxy data from the same core. We discuss the different possible drivers of their variability and argue that C<sub>24</sub> fatty acid  $\delta^{13}\text{C}$  predominantly reflects phytoplankton productivity in open water environments, while C<sub>18</sub> fatty acid  $\delta^{13}\text{C}$  reflects productivity in the marginal ice zone. These new proxies have implications for better understanding carbon cycle dynamics in the Antarctica coastal zone in future paleoclimate studies.

## 1 Introduction

Antarctic coastal zones are important players in the global carbon cycle. The deep ocean is ventilated in these regions as part of the Southern Ocean overturning circulation, allowing waters rich in nutrients and CO<sub>2</sub> to be upwelled to the surface. In the absence of biological activity, most of the CO<sub>2</sub> would be leaked to the atmosphere. However, coastal polynyas within the Antarctic margin are areas of very high primary productivity during the spring and summer months (e.g. Arrigo et al., 2008) that rapidly reduces CO<sub>2</sub> to low levels through photosynthesis (Arrigo and van Dijken, 2003; Arrigo et al., 2008), resulting in surface water CO<sub>2</sub> undersaturation with respect to atmospheric CO<sub>2</sub> (Tortell et al., 2011). The subsequent export and burial of the organic carbon produced during these intense phytoplankton blooms can significantly lower atmospheric CO<sub>2</sub> concentrations (Sigman and Boyle, 2000). Therefore, any change in the consumption of these nutrients by

41 phytoplankton, or any change in phytoplankton community structure, may affect the air-sea CO<sub>2</sub> exchange in  
42 this region.

43 Records of past phytoplankton productivity offer an opportunity to document the drivers of primary productivity  
44 at different timescales from pluri-decadal to millennial. In the Antarctic coastal zone past work has focused on  
45 records of organic carbon, biogenic silica and diatom abundances (Leccaroni et al., 1998; Frignani et al., 1998;  
46 Denis et al., 2009; Peck et al., 2015). These proxies however may provide a biased view of phytoplankton  
47 productivity as they only record a signal of siliceous productivity and may suffer from alteration during settling  
48 and burial (Beucher et al., 2004; Tréguer et al., 2017). As such, there is no robust understanding of how such  
49 records respond to surface water CO<sub>2</sub> which is of major importance in the context of Antarctic coastal sea ice  
50 changes.

51 Here we investigate the use of compound specific carbon isotope analysis ( $\delta^{13}\text{C}$ ) of free, saturated algal fatty  
52 acids (FAs) in marine sediments as a potential integrative proxy for reconstructing primary productivity in a  
53 polynya environment. Fatty acids have the potential to be a useful palaeoproductivity tool in this region due to  
54 their ubiquitous presence within marine sediments, while other commonly used compounds, such as alkenones,  
55 are absent. Fatty acids are also able to persist within the sediments for several thousand years, meaning they  
56 have the potential to be applied over long time spans in contrast to more labile compounds such as highly  
57 branched isoprenoid alkenes (HBIs). Furthermore, fatty acids are amenable to isotope analysis allowing them to  
58 yield more detailed information about the environment.

59 Previous studies in the highly-productive regions of the Southern Ocean have highlighted the potential for using  
60 compound-specific isotopes from algal biomarkers in sediments to track primary productivity changes both  
61 spatially and temporally. Villinski et al. (2008) found that the spatial variation in pCO<sub>2</sub> in the Ross Sea was  
62 associated with a variation in the  $\delta^{13}\text{C}$  of sedimentary organic carbon and sterol biomarkers, most likely due to a  
63 change in isotopic fractionation associated with the photosynthetic drawdown of CO<sub>2</sub>. Their results demonstrate  
64 that the spatial variation in surface water CO<sub>2</sub> is recorded in sedimentary organic matter and algal biomarkers.  
65 We explore this further as well as looking into other potential drivers of compound-specific carbon isotopes.

66 We use samples from core DTGC2011, a 4.69 m sediment core recovered from offshore Adélie Land, East  
67 Antarctica, spanning the last ~400 years. The core chronology is based on radiocarbon dates and confirmed by  
68 <sup>210</sup>Pb excess activity measurements, which indicate that DTGC2011 spans the 1580-2000 C.E. period with a  
69 mean sedimentation rate of ~1 cm yr<sup>-1</sup> (Supplementary Information S1). In order to understand the signal  
70 recorded by the FAs, we estimate the most likely biological source of these compounds and the habitat and  
71 season of production. Moreover, we compare downcore changes in FA concentrations and  $\delta^{13}\text{C}$  with other  
72 proxy data from the same core.

73

## 74 **Environmental setting**

75 The Adélie drift is located in the Dumont D'Urville Trough in the Adélie Basin, ca. 35 km offshore from Adélie  
76 Land (Fig. 1). This is a 1000 m deep, glacially scoured depression on the East Antarctic continental shelf,  
77 bounded to the east by the Adélie Bank. Sea ice plays a key role on the dynamics of the region, with both fast

78 ice and pack ice present off the coast of Adélie Land. A large bank of fast ice forms annually between 135 and  
79 142°E, and extends up to 120 km away from the coast (Massom et al., 2009). On the north edge of this fast ice  
80 buttress is an inlet of open water forming a polynya, an area of open water surrounded by sea ice (Bindoff et al.,  
81 2000).

82 The Adélie Coast is characterized by extremely high primary productivity, with phytoplankton assemblages  
83 dominated by diatoms (Beans et al., 2008). The site itself is located close to the Dumont D'Urville polynya  
84 (DDUP), with an annual net primary productivity (NPP) of 30.3 g C m<sup>-2</sup> a<sup>-1</sup>, but is also directly downwind and  
85 downcurrent of the much larger and highly productive Mertz Glacier polynya (MGP) to the east, with an annual  
86 NPP of 39.9 g C m<sup>-2</sup> a<sup>-1</sup> (Arrigo et al., 2015). Various factors are known to drive productivity trends in the  
87 Southern Ocean, including open water area, glacial melt and mixed layer depth (Arrigo et al., 2015). In the  
88 MGP, Arrigo (2007) found light and nutrient availability to be the most important factors, which will in turn be  
89 modulated by changes in mixed layer depth, ice cover and glacial ice melt. Physiological differences in  
90 *Phaeocystis antarctica* compared to diatoms mean it can thrive in lower nutrient conditions and lower CO<sub>2</sub>  
91 levels.

92 The region is affected by various water masses. High Salinity Shelf Water (HSSW) is formed on the shelf in  
93 coastal polynyas as a result of sea ice production and the associated brine rejection. HSSW flows out of the shelf  
94 through the Adélie sill at 143°E (Fig. 1). Modified Circumpolar Deep Water (mCDW) is a warm, macronutrient-  
95 rich and salty water mass which upwells onto the continental shelf through channels in the shelf break. mCDW  
96 has been observed to upwell across the shelf break near the Mertz Glacier at 144°E (Williams et al., 2008) (Fig.  
97 1). The Antarctic Coastal Current, also known as the East Wind Drift, flows westward often adjacent to ice  
98 shelves (Thompson et al., 2018). The Antarctic Surface Water (AASW) is a widespread water mass which  
99 extends across the continental shelf and has a surface mixed layer varying from a shallow (ca. 10 m), warmer  
100 and fresher layer in summer to a deeper (ca. 100 m), colder layer in winter. This is also transported westward  
101 along with the Antarctic Coastal Current (Martin et al., 2017). Surface waters along the Adélie coast have  
102 relatively high concentrations of nitrate, silica and phosphorus, with spatially variable levels of Fe which may be  
103 due to re-suspension of sediments and calving of ice (Vaillancourt et al., 2003; Sambrotto et al., 2003).

## 104 **2 Materials and Methods**

### 105 *Fatty acids*

106 One hundred and thirty-five sediment samples were taken for organic geochemical analyses, sampled at 1 cm  
107 intervals in the top 50 cm, 2 cm intervals between 50 and 100 cm, and 5 cm intervals until 458 cm. Lipid  
108 extractions were completed at the University of Birmingham using dichloromethane/methanol (3:1 v/v) and  
109 ultrasonication. The acid and neutral fractions were separated using an aminopropyl-silica gel column and the  
110 FAs eluted using diethyl ether with 4% acetic acid. The acid fraction was derivatized using boron trifluoride (14  
111 % in methanol (v/v)) and subsequently cleaned up using a silica gel column and the fatty acid methyl esters  
112 (FAMES) eluted with dichloromethane.

113 FAs were identified using an Agilent 7890B gas chromatograph (GC) coupled to an Agilent 5977A mass  
114 selective detector, with a BP5-MS (SGE) column (60m, 320µm internal diameter, 0.25µm film thickness).  
115 Helium was used as the carrier gas set at a constant flow rate of 2 ml/min. The MSD was run in scan mode with

116 a scan width of 50 to 800 mass units. Concentrations were quantified using an Agilent 7890B GC-flame  
117 ionization detector, using Hydrogen as the carrier gas with a constant flow rate of 2 ml min<sup>-1</sup>. An Rtx™-200  
118 column (105 m, 250µm internal diameter, 0.25µm film thickness) which has a  
119 poly(trifluoropropylmethylsiloxane) stationary phase was used for FA analyses to enable the best separation  
120 possible. The oven programme was: 70°C, held for 1 min, increased to 150°C at a rate of 30°C/min, increased to  
121 320°C at a rate of 3°C/min, then held for 10 minutes. FA concentrations were quantified by addition of a C19  
122 alkane as an internal standard, prepared in-house to the concentration of 10 ng/µl. The peak areas of FAs and the  
123 internal standard were used to calculate the concentration of each compound.

124 The δ<sup>13</sup>C composition of fatty acids are described in delta notation:

$$125 \quad \delta^{13}\text{C} (\text{‰}) = ((12\text{C}/13\text{C})_{\text{sample}} / (12\text{C}/13\text{C})_{\text{standard}} - 1) \times 1000$$

126 whereby the standard is Vienna Pee Dee Belemnite. Carbon isotopes were measured using an Agilent 7890A  
127 GC coupled to an Isoprime GC5 furnace and an Isoprime 100 isotope ratio mass spectrometer (IRMS). The  
128 Isoprime GC5 furnace contained a CuO furnace tube kept at 850°C. Helium was used as the carrier gas set at a  
129 constant flow of 1.7 ml/min and CO<sub>2</sub> was used as the reference gas. The GC had a VF-200ms column (60 m,  
130 250µm internal diameter, 0.25µm film thickness) which also has a poly(trifluoropropylmethylsiloxane)  
131 stationary phase. The oven programme was: 70°C, held for 1 min, increased to 150°C at a rate of 30°C/min,  
132 increased to 320°C at a rate of 3°C/min, then held for 5 minutes. Most samples were run using an Agilent 7693  
133 autosampler from dilutions of 10 – 100 µl. Where concentrations were very low, samples were dissolved in <10  
134 µl and were manually injected. Most samples were run in duplicate except for a few cases where the sample  
135 concentration was so low that the entire sample had to be injected in one run.

136 Machine performance was routinely checked using a FA ester mix (F8; Indiana University) containing eight FA  
137 compounds. This was run before the start of analysis and after every five duplicate samples. Errors are based on  
138 the difference between duplicate measures and are all within 0.26‰.

139 To correct for the additional carbon added during MeOH derivatization, three FA standards were analysed for  
140 their bulk carbon isotope value using an Elementar Pyrocube at the University of Birmingham. Samples were  
141 combusted at 920°C before being passed through a reduction column and the isotopic composition of sample  
142 gases was determined on an Isoprime continuous flow mass-spectrometer. These samples were then derivatized  
143 and then analysed on the GC-IRMS for the δ<sup>13</sup>C value of the FAME. The δ<sup>13</sup>C of the FA (δ<sup>13</sup>CFA) and FAME  
144 (δ<sup>13</sup>CFAME) were used to calculate the δ<sup>13</sup>C of the MeOH (δ<sup>13</sup>CMeOH) as follows:

$$145 \quad \delta^{13}\text{CMeOH} = (n\text{FAME} * \delta^{13}\text{CFAME}) - (n\text{FA} * \delta^{13}\text{CFA})$$

146 whereby nFAME is the number of carbons in the FAME and nFA is the number of carbons in the FA.

147 δ<sup>13</sup>CMeOH was calculated to be ca. -40.8‰ and the δ<sup>13</sup>CFAME values were corrected using:

$$148 \quad \delta^{13}\text{CFA} = ((n\text{FAME} * \delta^{13}\text{CFAME}) + 40.8) / n\text{FA}$$

149 *HBI*s

150 Two hundred and thirty-four samples were taken every 2 cm over the whole core for highly branched  
151 isoprenoids (HBI) alkenes analysis. HBIs were extracted at Laboratoire d'Océanographie et du Climat:  
152 Experimentations et Approches Numériques (LOCEAN), separately from the fatty acids, using a mixture of  
153 9mL CH<sub>2</sub>Cl<sub>2</sub>/MeOH (2:1, v:v). 7 hexyl nonadecane (m/z 266) was added as an internal standard during the first  
154 extraction steps, following the Belt et al (2007) and Massé et al. (2011) protocols. Several sonication and  
155 centrifugation steps were applied in order to fully extract the selected compounds (Etourneau et al., 2013). After  
156 drying with N<sub>2</sub> at 35°C, the total lipid extract was fractionated over a silica column into an apolar and a polar  
157 fraction using 3 mL hexane and 6 mL CH<sub>2</sub>Cl<sub>2</sub>/MeOH (1:1, v:v), respectively. HBIs were obtained from the  
158 apolar fraction following the procedures reported by Belt et al. (2007) and Massé et al. (2011). After removing  
159 the solvent with N<sub>2</sub> at 35°C, elemental sulfur was removed using the TBA (Tetrabutylammonium) sulfite  
160 method (Jensen et al., 1977; Riis and Babel, 1999). The obtained hydrocarbon fraction was analyzed within an  
161 Agilent 7890A gas chromatograph (GC) fitted with 30 m fused silica Agilent J&C GC column (0.25 mm i.d.,  
162 0.25 µm film thickness), coupled to an Agilent 5975C Series mass selective detector (MSD). Spectra were  
163 collected using the Agilent MS-Chemstation software. Individual HBIs were identified on the basis of  
164 comparison between their GC retention times and mass spectra with those of previously authenticated HBIs  
165 (Johns et al., 1999) using the Mass Hunter software. Values are expressed as concentration relative to the  
166 internal standard.

### 167 *Diatoms*

168 One hundred and eighteen samples were taken every 4 cm over the whole core for diatom analyses. Sediment  
169 processing and slide preparation followed the method described in Crosta et al. (2020). Diatom counting followed  
170 the rules described in Crosta and Koç (2007). Around 350 diatom valves were counted in each sample at a 1000X  
171 magnification on a Nikon Eclipse 80i phase contrast microscope. Diatoms were identified to species or species  
172 group level. Absolute abundances of diatoms were calculated following the equation detailed in Crosta et al.  
173 (2008). The relative abundance of each species was determined as the fraction of diatom species against total  
174 diatom abundance in the sample.

### 176 **3 Fatty acids within DTGC2011**

177 Analysis by GC-MS identified seven dominant saturated FAs within the DTGC2011 samples (Fig. S2). These  
178 have carbon chain lengths of C<sub>16</sub> to C<sub>26</sub> and only the saturated forms (i.e. no double bonds) were identified.  
179 These are predominantly even chain length FAs, with only minor amounts of the C<sub>17</sub> compound measured  
180 (Gilchrist, 2018).

#### 181 **3.1 Fatty acid concentration**

182 The C<sub>19</sub> alkane was used as an internal standard to aid quantification of fatty acid concentrations. However, it  
183 should be noted that since this standard was added to samples post-extraction, our concentration estimates are  
184 semi-quantitative but can be used to compare concentration changes in different FA compounds.

185 Down core analysis of FA concentrations reveals clear groupings in concentration changes. In the upper part of  
186 the core (ca. 3 – 90 cm depth), spanning the last ~78 years, all FA compounds show a similar pattern, with

187 elevated concentrations, broadly decreasing down-core (Fig. 2). Below this, however, two groups clearly  
188 diverge. These can be broadly divided into short-chained fatty acids (C<sub>16</sub> to C<sub>20</sub>; SCFAs) and long-chained fatty  
189 acids (C<sub>22</sub> to C<sub>26</sub>; LCFAs). Within these groups, the concentrations of different compounds show similar trends,  
190 but the two groups (SCFAs vs LCFAs) show different trends to each other (Gilchrist, 2018). This is confirmed  
191 by R<sup>2</sup> values calculated for the linear regression of concentrations of each FA against each other throughout the  
192 core (Fig. 3; n = 135, p < 0.001). Correlations between the SCFAs have R<sup>2</sup> values between 0.97 and 0.99, while  
193 R<sup>2</sup> values of LCFAs range between 0.88 and 0.95. Between the two groups, however, R<sup>2</sup> values are all lower,  
194 ranging between 0.50 and 0.77.

195 These distinct groupings suggest that compounds within each group (SCFAs and LCFAs) likely have a common  
196 precursor organism or group of organisms, but the two groups themselves have different producers from each  
197 other. These producers may in turn thrive during different seasons or within different habitats and thus, the  
198 isotopic composition of compounds from these different groups may record different environmental signals.

199 R<sup>2</sup> values were also calculated for samples below 25 cm only (ca. 1587 – 1978 C.E.), to remove correlations  
200 associated with preservation changes in the top part of the core (discussed below). Although the R<sup>2</sup> values are  
201 not quite as high, they broadly confirm these groupings, with the R<sup>2</sup> values generally being greater within the  
202 two groups (n = 73). R<sup>2</sup> values range from 0.93 for the C<sub>18</sub> with C<sub>20</sub>, down to 0.07 for the C<sub>18</sub> and C<sub>24</sub> (Fig. 4).

203 The C<sub>18</sub> and C<sub>24</sub> FAs are the most abundant compounds within the SCFA and LCFA groups, respectively, and  
204 also the least correlated with each other both in the whole core (R<sup>2</sup> = 0.5) and below 25 cm (R<sup>2</sup> = 0.07), which  
205 suggests they are the most likely to be produced by different organisms. Furthermore, these two compounds  
206 yielded the highest quality isotope measurements, due to their greater concentrations, clean baseline and  
207 minimal coeluting peaks (Fig. S2). Thus, these two compounds (C<sub>18</sub> and C<sub>24</sub>) will be the focus of analysis and  
208 discussion.

209

### 210 **3.2 Potential sources of the C<sub>18</sub> fatty acid**

211 Potential sources for the C<sub>18</sub> FA in core U1357 (recovered from the same site as DTGC2011) are discussed in  
212 Ashley et al. (*in press*) who suggest the prymnesiophyte *Phaeocystis antarctica* to be the most likely main  
213 producer. This is based on a) previous studies of FAs produced by microalgae (Dalsgaard et al., 2003), b) the  
214 high observed abundance of *P. antarctica* within modern Adélie surface waters (Riaux-Gobin et al., 2011;  
215 Sambrotto et al; 2003) and c) comparison between the measured δ<sup>13</sup>C values and those reported in the literature  
216 for *P. antarctica* (Kopczynska et al., 1995; Wong and Sackett, 1978). Unfortunately, the absence of *P.*  
217 *antarctica* in sediments, as it does not biomineralize any test, precludes the direct comparison of down core  
218 trends of this species with FAs. *Phaeocystis antarctica* has been found to live within and underneath sea ice  
219 before its break up, as well as in open ocean waters (Riaux-Gobin et al., 2013; Poulton et al., 2007), due to its  
220 ability to use a wide range of light intensities for energy production (Moisan and Mitchell, 1999).

221 Furthermore, Skerratt et al. (1998) compared the FAs produced by *P. antarctica* and two Antarctic diatoms, in  
222 culture samples, and showed that *P. antarctica* produced a much higher percentage of both saturated FAs (C14-  
223 C20) and C18 FAs than the diatoms. This supports the hypothesis of *P. antarctica* being a dominant and

224 abundant source of the saturated C<sub>18</sub> FA in the Adélie basin though minor contributions of C<sub>18</sub> from other  
225 phytoplankton species such as the diatoms and dinoflagellates cannot be excluded.

### 226 **3.3 Potential sources of the C<sub>24</sub> fatty acid**

227 Long-chain *n*-alkyl compounds, including FAs, are major components of vascular plant waxes and their  
228 presence within sediments has commonly been used as a biomarker of terrestrial plants (Pancost and Boot,  
229 2004). Although plants such as bryophytes (e.g. mosses) which are present in the Antarctic do also produce  
230 LCFAs (Salminen et al., 2018), it is unlikely that FAs from terrestrial plants make a significant contribution to  
231 the water column, due to their extremely limited extent on the continent, and the significant distance of the site  
232 from other continental sources.

233 However, there is much evidence in the literature for various aquatic sources of LCFAs, a few of which are  
234 summarized in Table S2. Although not all of these sources are likely to be present within the coastal waters  
235 offshore Adélie Land, it highlights the wide range of organisms which can produce these compounds, and thus  
236 suggests that an autochthonous marine source is likely, especially considering the highly productive nature of  
237 this region.

### 238 **3.4 Microbial degradation and diagenetic effects on fatty acid concentration**

239 Both the C<sub>18</sub> and C<sub>24</sub> FAs show an overall decrease in concentrations down-core, with significantly higher  
240 concentrations in the top 80 cm (representing ~70 years) compared to the rest of the core. Below this point, FAs  
241 concentrations variations are attenuated (Fig. 2).

242 Many studies have shown that significant degradation of FAs occurs both within the water column and surface  
243 sediments as a result of microbial activity, and that there is preferential break down of both short-chained and  
244 unsaturated FA, compared to longer-chained and saturated FA (Haddad et al., 1992; Matsuda, 1978; Colombo et  
245 al., 1997). Haddad et al. (1992) studied the fate of FAs within rapidly accumulating (10.3 cm yr<sup>-1</sup>) coastal  
246 marine sediments (off the coast of North Carolina, USA) and showed that the vast majority (ca. 90%) of  
247 saturated FAs were lost due to degradation within the top 100 cm (representing ~10 years). Similarly, Matsuda  
248 and Koyama (1977) found FA concentrations decrease rapidly within the top 20 cm of sediment (accumulating  
249 at 4 mm yr<sup>-1</sup>) from Lake Suwa, Japan. Assuming similar processes apply to the DTGC2011 sediments, this  
250 suggests the declining concentrations within the upper part of the core are largely the result of diagenetic effects  
251 such as microbial activity occurring within the surface sediments, and thus do not reflect a real change in  
252 production of these compounds in the surface waters.

253 The complete lack of both unsaturated and short chained (fewer than 16 carbon atoms) FA compounds  
254 identified within DTGC2011 samples, even within the top layers, suggests that selective breakdown of  
255 compounds has already occurred within the water column and on the sea floor (before burial). Wakeham et al.  
256 (1984) assessed the loss of FAs with distance during their transport through the water column at a site in the  
257 equatorial Atlantic Ocean and estimated that only 0.4 to 2% of total FAs produced in the euphotic zone reached  
258 a depth of 389 m, and even less reaching more than 1,000 m depth, the vast majority of material being recycled  
259 in the upper water column. Their results also show a significant preference for degradation of both unsaturated  
260 and short chained compounds over saturated and longer chain length compounds. Although no studies into the  
261 fate of lipids within the water column exist for the Adélie region, the >1,000 m water depth at the core site

262 would provide significant opportunity for these compounds to be broken down during transportation through the  
263 water column. It is likely, therefore, that the distribution of compounds preserved within the sediments will not  
264 be a direct reflection of production in the surface waters, and explains the preference for saturated FAs with  
265 carbon chain lengths of 16 and more.

266 Although FA concentrations in the top 80 cm of core DTGC2011 are much higher overall than the sediments  
267 below and show a broad decline over this section, there is a high level of variability. Concentrations do not  
268 decrease uniformly within the top part of the core, as may be expected if concentration change is a first order  
269 response to declining microbial activity. The peak in total FAs instead occurs at a depth of 21-22 cm with a  
270 concentration more than an order of magnitude higher than in the top layer. This variability creates difficulty in  
271 directly determining the effects of diagenesis. However, by 25 cm (ca. 1978 C.E.) the concentrations drop to  
272 below 1,000 ng g<sup>-1</sup> and remain so until 32 cm before increasing again. This may suggest that diagenetic effects  
273 of FA concentrations are largely complete by 25 cm (representing ca. 25 years), consistent with results from  
274 Haddad et al. (1992) and Matsuda and Koyama (1977), and that subsequent down-core concentration variations  
275 predominantly represent real changes in export productivity, resulting from environmental factors. However, the  
276 fluctuating nature of concentrations particularly in the youngest sediments means it is difficult to clearly unpick  
277 the effects of diagenesis from actual changes in production of these compounds, and a clear cut-off point for  
278 diagenetic effects cannot be determined.

### 279 **3.5 Comparison of fatty acid concentrations with highly branched isoprenoid alkenes**

280 We compare FA concentrations with other organic compounds (whose source is better constrained) in  
281 DTGC2011 to better understand FA sources. Direct comparison between different organic compound classes  
282 can be made since both are susceptible to similar processes of diagenesis, in contrast to other proxies such as  
283 diatoms. In core DTGC2011, concentrations of di- and tri-unsaturated highly branched isoprenoid (HBI) alkenes  
284 (referred to as HBI diene and HBI triene, respectively hereafter) were available.

285 In Antarctic marine sediments HBIs have been used as a tool for reconstructing sea ice (Belt et al., 2016, 2017).  
286 Smik et al. (2016) compared the concentrations of HBIs in sediment samples offshore East Antarctica from the  
287 permanently open-ocean zone (POOZ), the marginal ice zone (MIZ) and the summer sea-ice zone (SIZ). They  
288 found the HBI diene reached the highest concentrations in the SIZ and was absent from the POOZ. In contrast,  
289 the HBI triene was most abundant in the MIZ, i.e. at the retreating sea ice edge, with much lower concentrations  
290 in the SIZ and POOZ. This suggests that the two compounds are produced in contrasting environments but  
291 remain sensitive to changes in sea ice.

292 The HBI diene biomarker (or IPSO<sub>25</sub> for Ice Proxy Southern Ocean with 25 Carbons) is mainly biosynthesised  
293 by *Berkeleya adeliensis* (Belt et al., 2016), a diatom which resides and blooms within the sea ice matrix, and  
294 thus can be used as a proxy for fast ice attached to the coast. In contrast, the presence of the HBI triene mostly in  
295 the MIZ is suggestive of a predominantly pelagic phytoplankton source (e.g. *Rhizosolenia* spp, Massé et al.,  
296 2011; Smik et al., 2016; Belt et al., 2017), rather than sea-ice dwelling diatoms (Smik et al., 2016). The fact that  
297 HBI triene reached its greatest abundance within the MIZ suggests its precursor organism may thrive in the  
298 stratified, nutrient-rich surface waters of the sea-ice edge.



299 One key similarity between both the HBI diene and triene, and the FA concentrations is that the highest  
300 concentrations are found in the youngest sediments. These compounds all show broad increases in concentration  
301 from 110 cm depth (ca. 1900 C.E) until the top of the core (Fig. 2 and 5). Concentrations of HBIs are also  
302 susceptible to degradation through the water column through visible light induced photo-degradation (Belt and  
303 Müller, 2013) and diagenetic effects within these sediments including sulphurisation (Sinninghe Damsté et al.,  
304 2007), isomerisation and cyclisation (Belt et al., 2000). Thus, it is likely that the elevated concentrations, and  
305 thus the similarity between FA and HBI concentrations, is due to the material being fresher and thus less  
306 affected by diagenesis, with diagenetic effects having an increasing and progressive impact down to ca. 25cm  
307 depth.

308 However, despite an overall increase in HBI and FA concentrations above 110 cm depth, there are clear  
309 deviations from this trend. Concentrations of the HBI triene show some broad similarities with FA  
310 concentrations. In particular, both the HBI triene and the C<sub>18</sub> FA have coeval concentration peaks around 1980-  
311 88, 1967, 1938, 1961-72, 1848 and 1752 C.E. (Fig. 5). These peaks are offset from the HBI diene  
312 concentrations, suggesting that they result from increased production in the surface waters rather than simply  
313 changes in preservation. The HBI triene is more susceptible to degradation than the diene (Cabedo Sanz et al.,  
314 2016), so while this could explain some of the differences between the diene and triene records, where the triene  
315 increases independently of the diene, this is likely to be a genuine reflection of increased production of these  
316 compounds at the surface rather than an artefact of preservation processes.

317 This close similarity between the C<sub>18</sub> FA and HBI triene concentrations (Fig. 5) suggests that the C<sub>18</sub> may also  
318 be produced by an organism associated with the retreating ice edge. *Phaeocystis antarctica* has been proposed  
319 as a potential producer of the C<sub>18</sub> in core U1357B (Ashley et al., *in review*). In the Ross Sea, *P. antarctica* has  
320 been observed to dominate the phytoplankton bloom during the spring, blooming in deep mixed layers as the sea  
321 ice begins to melt, after which diatoms tend to dominate during the summer (Arrigo et al., 1999; Tortell et al.,  
322 2011; DiTullio et al., 2000). However, a few studies in the Adélie region suggest this is not the case there.  
323 Offshore Adélie Land, *P. antarctica* has been found to only appear late in the spring/early summer, later than  
324 many diatom species. During this time, it occurs preferentially within the platelet ice and under-ice water  
325 (Riaux-Gobin et al., 2013). Furthermore, Sambrotto et al. (2003) observed a surface bloom of *P. antarctica* near  
326 the Mertz Glacier (Fig. 1) during the summer months, in very stable waters along the margin of fast ice and  
327 Riaux-Gobin et al. (2011) found *P. antarctica* to be abundant in the coastal surface waters eight days after ice  
328 break up. This indicates an ecological niche relationship with cold waters and ice melting conditions. This might  
329 explain the close similarity between the C<sub>18</sub> and HBI triene concentrations, both produced by organisms  
330 occupying a similar habitat at the ice edge.

331 The C<sub>24</sub> FA record also shows some similarity with the HBI triene record. This appears to be mostly in the top  
332 part of the core where the highest concentrations are found. The reason for this resemblance is unclear,  
333 especially considering the lack of correlation between the C<sub>24</sub> and C<sub>18</sub> FA concentrations. However, it may relate  
334 to the progressive effect of diagenesis through the core. There is less similarity between the C<sub>24</sub> and both the  
335 HBI triene also HBI diene, (compared to the coherence between C<sub>18</sub> FA and HBI triene), which suggests that  
336 the C<sub>24</sub> FA is predominantly produced by an organism which is not associated with sea ice, and thus instead  
337 with more open waters. Seventy-three diatom species were encountered in core DTGC2011 (Campagne, 2015),

338 with *Fragilariopsis curta* and *Chaetoceros* resting spores being the most abundant. However, trends in diatom  
339 abundances do not show any clear correlations with the C<sub>18</sub> or C<sub>24</sub> FA concentrations. While this would lend  
340 support to the hypothesis that diatoms are not the main producers of these compounds, the differing effects of  
341 diagenesis on the preservation of diatoms and lipids could also explain some of the differences in observed  
342 concentrations, particularly in the upper part of the core. The known producer of the HBI diene, *Berkeleya*  
343 *adeliensis*, for example, was not recorded within the core, likely due to their lightly silicified frustules which are  
344 more susceptible to dissolution (Belt et al., 2016). Therefore, despite the lack of a correlation between diatom  
345 abundances and FA concentrations, we cannot entirely rule out the possibility of a minor contribution of FAs by  
346 diatoms.

#### 347 4 Carbon isotopes of fatty acids

348 Down-core changes in  $\delta^{13}\text{C}$  for the C<sub>18</sub> and C<sub>24</sub> FA ( $\delta^{13}\text{C}_{18\text{FA}}$  and  $\delta^{13}\text{C}_{24\text{FA}}$ , respectively) (Fig. 7) clearly show  
349 different trends, with very little similarity between them ( $R^2 = 0.016$ ). This further supports the idea that these  
350 compounds are being produced by different organisms, and thus are recording different information.

351 The mean carbon isotope value of  $\delta^{13}\text{C}_{18\text{FA}}$  of -29.8 ‰ in core U1357 from the same site (Ashley et al., *in*  
352 *review*) is suggestive of a pelagic phytoplankton source (Budge et al., 2008). In core DTGC2011 the mean  
353 values of  $\delta^{13}\text{C}_{18\text{FA}}$  and  $\delta^{13}\text{C}_{24\text{FA}}$  are -26.2 ‰ and -27.6 ‰, respectively. Though more positive, these values are  
354 still within the range of a phytoplankton source. Additionally, we tentatively suggest that the 0.5‰ more  
355 positive  $\delta^{13}\text{C}_{18\text{FA}}$  mean value over the  $\delta^{13}\text{C}_{24\text{FA}}$  may indicate the contribution of sea-ice dwelling algae  
356 producers, since carbon fixation occurring within the semi-closed system of the sea ice will lead to a higher  
357 degree of CO<sub>2</sub> utilisation than in surrounded open waters (Henley et al., 2012). Although no studies on FA  $\delta^{13}\text{C}$   
358 of different organisms are available for the Southern Ocean, Budge et al. (2008) measured the mean  $\delta^{13}\text{C}$  value  
359 of C<sub>16</sub> FA from Arctic sea-ice algae (-24.0 ‰) to be 6.7 ‰ higher than pelagic phytoplankton (-30.7 ‰) from  
360 the same region.

361 The higher  $\delta^{13}\text{C}$  of the C<sub>18</sub> FA could therefore be indicative of *P. antarctica* living partly within the sea ice, e.g.  
362 during early spring before ice break up. The more negative  $\delta^{13}\text{C}_{24\text{FA}}$  suggests it is more likely to be produced by  
363 phytoplankton predominantly within open water.

#### 364 4.1 Controls on $\delta^{13}\text{C}_{\text{FA}}$

365 The  $\delta^{13}\text{C}_{18\text{FA}}$  record shows a broadly increasing trend towards more positive values from ca. 1587 until ca. 1920  
366 C.E., with short term fluctuations of up to ~4 ‰ superimposed on this long-term trend (Fig. 7). This is followed  
367 by a period of higher variability with a full range of 5.6 ‰ until the most recent material (ca. 1999 C.E.), with  
368 more negative  $\delta^{13}\text{C}$  values between 1921 and 1977 C.E. and a rapid shift toward more positive values thereafter.  
369 In contrast, the  $\delta^{13}\text{C}_{24\text{FA}}$  record overall shows a weak, negative trend, with large decadal fluctuations of up to 4.6  
370 ‰, with a more pronounced negative trend after ca. 1880 C.E. (Fig. 7).

371 Below we consider the various factors which may control the carbon isotope value of algal biomarkers produced  
372 in the surface waters. Down-core changes in FA  $\delta^{13}\text{C}$  are likely to be a function of either the  $\delta^{13}\text{C}$  of the  
373 dissolved inorganic carbon (DIC) source, changes in the species producing the biomarkers, diagenesis or

374 changing photosynthetic fractionation ( $\epsilon_p$ ). The next section outlines the potential influence of these factors may  
375 have in order to assess the mostly likely dominant driver of FA  $\delta^{13}\text{C}$ .

#### 376 *4.1.1 Isotopic composition of DIC*

377 The  $\delta^{13}\text{C}$  of the DIC source can be affected by upwelling or advection of different water masses, or the  $\delta^{13}\text{C}$  of  
378 atmospheric  $\text{CO}_2$ . Around the Antarctic, distinct water masses have unique carbon, hydrogen and oxygen  
379 isotope signatures and thus isotopes can be used as water mass tracers (e.g. Mackensen, 2001, Archambeau et  
380 al., 1998). In the Weddell Sea for example, Mackensen (2001) determined the  $\delta^{13}\text{C}$  value of eight water masses,  
381 which ranged from 0.41 ‰ for Weddell Deep Water, sourced from CDW, to 1.63 ‰ for AASW. A similar  
382 range of  $\sim 1.5$  ‰ was identified in water masses between the surface and  $\sim 5,500$  m depth along a transect from  
383 South Africa to the Antarctic coast (Archambeau et al., 1998). Assuming similar values apply to these water  
384 masses offshore Adélie Land, this range in values would be insufficient to explain the  $\sim 5$  ‰ variation of  $\delta^{13}\text{C}$   
385 recorded by both  $\text{C}_{18}$  and  $\text{C}_{24}$  FA, even in the situation of a complete change in water mass over the core site.  
386 Furthermore, site DTGC2011, located within a 1,000 m deep depression and bounded by the Adélie Bank to the  
387 north, is relatively sheltered from direct upwelling of deep water (Fig. 1). Though inflow of mCDW has been  
388 shown to occur within the Adélie Depression to the east of the bank (Williams and Bindoff, 2003) and possibly  
389 within the Dumont d'Urville Trough, only very small amplitude changes in  $\delta^{13}\text{C}$  of benthic foraminifera,  
390 tracking upper CDW, have been observed over the Holocene in Palmer Deep, West Antarctica (Shevenell and  
391 Kennett, 2002). Although from a different location, this argues against large changes in the isotopic composition  
392 of the source of mCDW.

393 Changes in the  $\delta^{13}\text{C}$  of atmospheric  $\text{CO}_2$ , which is in exchange with the surface waters could also have the  
394 potential to drive changes in the  $\delta^{13}\text{C}$  of algal biomarkers. Over the last ca. 200 years, the anthropogenic burning  
395 of fossil fuels has released a large amount of  $\text{CO}_2$  depleted in  $^{13}\text{C}$ , meaning that the  $\delta^{13}\text{C}$  of  $\text{CO}_2$  has  
396 decreased by ca. 1.5 ‰, as recorded in the Law Dome ice core. Prior to this, however, the  $\delta^{13}\text{C}$  of  $\text{CO}_2$  in the  
397 atmosphere remained relatively stable, at least for the last thousand years (Francey et al., 1999). Therefore, this  
398 could potentially drive the  $\delta^{13}\text{C}$  of algal biomarkers towards more negative values within the last 200 years, but  
399 this could not explain the full variation of  $\sim 5$ -6 ‰ in FA  $\delta^{13}\text{C}$  measured throughout the core. Although the  $\text{C}_{24}$   
400  $\delta^{13}\text{C}$  shows a slight decrease over the last ca. 100 years, this is preceded by increasing  $\delta^{13}\text{C}$ , while the  $\text{C}_{18}$   $\delta^{13}\text{C}$   
401 displays no clear trend over the last 200 years. If atmospheric  $\text{CO}_2$  was a key driver of fatty acid  $\delta^{13}\text{C}$ , we would  
402 expect both compounds to respond together, showing a trend towards more negative values over the last 200  
403 years which neither of them do. This suggests that the effect of changing  $\delta^{13}\text{C}$  of atmospheric  $\text{CO}_2$  is  
404 insignificant compared to local and regional inter-annual variations as a result of other environmental drivers  
405 (discussed below).

#### 406 *4.1.2 Changing species*

407 A shift in the organisms producing the FA could also affect  $\delta^{13}\text{C}$  where species have different fractionation  
408 factors. For example, changing diatom species have been shown to have an effect on bulk organic matter  $\delta^{13}\text{C}$  in  
409 core MD03-2601, offshore Adélie Land, over the last 5 ka (Crosta et al., 2005). However, the bulk organic  
410 matter might have contained other phytoplankton groups than diatoms with drastically different  $\delta^{13}\text{C}$  values and  
411 fractionation factors. Here we measured  $\delta^{13}\text{C}$  of individual biomarkers, produced by a more restricted group of  
412 phytoplankton groups (possibly restricted to a few dominant species) compared to bulk  $\delta^{13}\text{C}$ . As discussed

413 above, the C<sub>18</sub> appears to be produced predominantly by *P. antarctica*, whereas diatoms do not tend to produce  
414 high proportions of this compound (Dalsgaard et al., 2003).

#### 415 4.1.3 Effect of diagenesis on lipid $\delta^{13}\text{C}$

416 Sun et al. (2004) studied the carbon isotope composition of FAs during 100 days of incubation in both oxic and  
417 anoxic seawater. They observed a shift towards more positive values in FA  $\delta^{13}\text{C}$ , ranging between 2.6 ‰ for the  
418 C<sub>14:0</sub> and as much as 6.9‰ in the C<sub>18:1</sub>, under anoxic conditions. This suggests that diagenesis could affect FA  
419  $\delta^{13}\text{C}$  in core DTGC2011. However, these observed changes are rapid (days to months), occurring on timescales  
420 which are unresolvable in the FA  $\delta^{13}\text{C}$  record (annual to decadal), and thus may have no effect on the trends  
421 observed in our record. Based on concentration data discussed above, it seems that diagenetic overprint is  
422 largely complete by ~25 cm (Fig. 2). In the top 25 cm of the core (ca. 1978 – 1998 C.E.), the  $\delta^{13}\text{C}_{24\text{FA}}$  values  
423 increase by ~2.5 ‰, downward ( $R^2 = 0.63$ ,  $n = 11$ ) while the  $\delta^{13}\text{C}_{18\text{FA}}$  values display a large variation with no  
424 overall trend ( $R^2 = 0.12$ ,  $n = 20$ ). If diagenesis was driving the changes in  $\delta^{13}\text{C}$ , it is likely that this trend would  
425 be observed in all FA compounds.

426 Taken together, it appears that neither changes in the  $\delta^{13}\text{C}$  of the DIC, changing phytoplankton groups nor  
427 diagenesis can fully explain the variation of FA  $\delta^{13}\text{C}$  recorded within DTGC2011. Therefore, we hypothesise  
428 that changes in  $\epsilon_p$  are the main driver of FA  $\delta^{13}\text{C}$ .

#### 429 4.2 Controls on photosynthetic fractionation ( $\epsilon_p$ )

430 There is a positive relationship between  $\epsilon_p$  in marine algae and dissolved surface water CO<sub>2(aq)</sub> concentration  
431 (Rau et al., 1989). As a result, higher  $\delta^{13}\text{C}$  values are hypothesised to reflect lower surface water CO<sub>2(aq)</sub> and vice  
432 versa. Popp et al. (1999) showed a strong negative correlation between CO<sub>2(aq)</sub> and  $\delta^{13}\text{C}$  of suspended  
433 particulate organic matter across a latitudinal transect in the Southern Ocean, suggesting that changes in surface  
434 water CO<sub>2(aq)</sub> can explain a large amount of the variation in  $\delta^{13}\text{C}$ . Changes in surface water CO<sub>2(aq)</sub>  
435 concentration in turn may be driven by various factors, including changing atmospheric CO<sub>2</sub> (Fischer et al.,  
436 1997), wind-driven upwelling of deep, carbon-rich water masses (Sigman and Boyle, 2000; Takahashi et al.,  
437 2009), sea-ice cover (Henley et al., 2012) and/or primary productivity (Villinski et al., 2008). Thus, determining  
438 the main driver(s) of surface water CO<sub>2</sub> changes offshore Adélie Land should enable interpretation of the  
439 DTGC2011 FA  $\delta^{13}\text{C}$  records.

#### 440 4.2.1 Sea ice

441 Brine channels within sea ice have very low CO<sub>2</sub> concentrations and a limited inflow of seawater. Carbon  
442 isotopic fractionation of algae living within these channels has been shown to be greatly reduced compared to  
443 organisms living in the surrounding open waters (Gibson et al., 1999), leading to elevated  $\delta^{13}\text{C}$  values. It is thus  
444 possible that, under conditions of high sea-ice cover, enhanced FA contribution from sea-ice algae leads to  
445 elevated sedimentary  $\delta^{13}\text{C}$  values. HBI diene concentrations within DTGC2011 show a much greater presence  
446 of fast ice at the core site ca. 1960 C.E (Fig. 5). However, during this time there is no clear elevation in  $\delta^{13}\text{C}$   
447 concentrations in either  $\delta^{13}\text{C}_{18\text{FA}}$  or  $\delta^{13}\text{C}_{24\text{FA}}$ , both instead showing generally lower  $\delta^{13}\text{C}$  values. In fact,  $\delta^{13}\text{C}_{18\text{FA}}$   
448 shows the lowest values of the whole record between 1925 and 1974 C.E., during which sea ice, as recorded by  
449 the HBI diene, is at its highest level. This suggests that inputs in sea-ice algae at this time are not driving  
450 changes in FA  $\delta^{13}\text{C}$ .

451 The DTGC2011 core site sits proximal to the Dumont D'Urville polynya, which has a summer area of  $13.02 \times$   
452  $10^3 \text{ km}^2$  and a winter area of  $0.96 \times 10^3 \text{ km}^2$  (Arrigo and van Dijken, 2003). Changes in the size of the polynya  
453 both on seasonal and inter-annual time scales will affect air-sea  $\text{CO}_2$  exchange and thus also surface water  $\text{CO}_2$   
454 concentration. A reduced polynya may lead to greater supersaturation of  $\text{CO}_2$  in the surface waters due to  
455 reduced outgassing, allowing  $\text{CO}_2$  to build up below the ice, leading to lower  $\delta^{13}\text{C}$  values of algal biomarkers  
456 produced in that habitat (Massé et al., 2011). Thus changes in the extent of sea ice may also effect FA  $\delta^{13}\text{C}$ .

#### 457 *4.2.2 Observed trends in surface water $\text{CO}_{2(\text{aq})}$*

458 If the trend in surface water  $\text{CO}_{2(\text{aq})}$  paralleled atmospheric  $\text{CO}_2$ , with an increase of over 100 ppm over the last  
459 200 years (MacFarling Meure et al., 2006), we might expect phytoplankton to exert a greater fractionation  
460 during photosynthesis in response to elevated surface water  $\text{CO}_{2(\text{aq})}$  concentration, resulting in more negative  
461  $\delta^{13}\text{C}$  values. Taking into account the decline in atmospheric  $\delta^{13}\text{C}$  over the same period would further enhance  
462 the reduction in phytoplankton  $\delta^{13}\text{C}$ . Fischer et al. (1997) looked at the  $\delta^{13}\text{C}$  of both sinking matter and surface  
463 sediments in the South Atlantic and suggested that, since the preindustrial, surface water  $\text{CO}_{2(\text{aq})}$  has increased  
464 much more in the Southern Ocean than in the tropics. They estimated that a 70 ppm increase in  $\text{CO}_{2(\text{aq})}$  in  
465 surface waters of  $1^\circ\text{C}$  would decrease phytoplankton  $\delta^{13}\text{C}_{\text{org}}$  by ca. 2.7‰, and up to 3.3‰  $\delta^{13}\text{C}$  change are  
466 included, between preindustrial and 1977-1990. However, sea ice cover and summer primary productivity are  
467 likely to be much higher off Adélie Land than in the South Atlantic, both of which will affect air-sea gas  
468 exchange.

469 Shadwick et al. (2014) suggest that surface water  $\text{CO}_2$  should track the atmosphere in the Mertz Polynya region,  
470 despite the seasonal ice cover limiting the time for establishing equilibrium with the atmosphere. They  
471 calculated wintertime  $\text{CO}_2$  in the shelf waters of the Mertz Polynya region, offshore Adélie Land (Fig. 1),  
472 measuring ca. 360 ppm in 1996, ca. 396 ppm in 1999, and ca. 385 ppm in 2007, while atmospheric  $\text{CO}_2$  at the  
473 South Pole was 360, 366 and 380 ppm, respectively (Keeling et al., 2005). Based on the 1996 and 2007 data  
474 only, an increase in  $\text{CO}_2$  of ca. 25 ppm is observed over these 11 years, coincident with the 20 ppm atmospheric  
475  $\text{CO}_2$  increase over this time period. However, high interannual variability ( $\pm$  ca. 30 ppm) is evident (e.g. 396  
476 ppm in 1999) suggesting that other factors, particularly upwelling, may override this trend. The latter was also  
477 suggested by Roden et al. (2013) based on winter surface water measurements in Prydz Bay, indicating that  
478 decadal-scale carbon cycle variability is nearly twice as large as the anthropogenic  $\text{CO}_2$  trend alone.

479 During the austral winter, upwelling of deep water masses causes  $\text{CO}_2$  to build up in the surface waters, and sea  
480 ice cover limits gas exchange with the atmosphere (Arrigo et al., 2008; Shadwick et al., 2014). Although only  
481 limited data, the measurements by Shadwick et al. (2014) suggest slight supersaturation, of up to 30 ppm, occurs  
482 in the winter due to mixing with carbon-rich subsurface water, but with high interannual variability. This is  
483 compared to undersaturation of 15 to 40 ppm during the summer as a result of biological drawdown of  $\text{CO}_2$ .  
484 Roden et al. (2013) also observed varying levels of winter supersaturation in Prydz Bay, East Antarctica, with  
485 late winter  $\text{CO}_2$  values of 433 ppm in 2011 (45  $\mu\text{atm}$  higher than atmospheric  $\text{CO}_2$ ), and suggested that  
486 intrusions of C-rich mCDW onto the shelf may play a part in this. Similarly, winter surface water  $\text{CO}_2$  of 425  
487 ppm has been measured by Sweeney (2003) in the Ross Sea, before being drawn down to below 150 ppm in the  
488 summer as phytoplankton blooms develop.

489 Enhanced upwelling of deep carbon-rich waters in the Southern Ocean are thought to have played a key role in  
490 the deglacial rise of atmospheric CO<sub>2</sub>, increasing CO<sub>2</sub> concentrations by ~80 ppm (Anderson et al., 2009; Burke  
491 and Robinson, 2012). Changes in upwelling offshore Adélie Land could therefore drive some interannual  
492 variability in surface water CO<sub>2</sub> and hence FA δ<sup>13</sup>C in DTGC2011. However, upwelling tends to be stronger  
493 during the winter months, when sea-ice formation and subsequent brine rejection drive mixing with deeper C-  
494 rich waters. At this time, heavy sea-ice cover limits air-sea gas exchange and enhances CO<sub>2</sub> supersaturation in  
495 regional surface waters (Shadwick et al., 2014). In contrast, the phytoplankton producing FA thrive during the  
496 spring and summer months during which CO<sub>2</sub> is rapidly drawn down and the surface waters become  
497 undersaturated. However, upwelling cannot be discarded as a possible contributor to surface water CO<sub>2</sub> change.  
498 However, the core site is in a relatively sheltered area and is probably not affected by significant upwelling.

499 Based on these studies, changes in atmospheric CO<sub>2</sub> concentration and δ<sup>13</sup>C of the source appear to be unlikely  
500 to be a dominant driver of the FA δ<sup>13</sup>C record, with interannual variations driven by other factors overriding any  
501 longer-term trend. There is also no clear anthropogenic decline in the FA δ<sup>13</sup>C record over the last 200 years,  
502 which supports this hypothesis.

#### 503 *4.2.3 Productivity*

504 Given that changes in atmospheric CO<sub>2</sub>, source signal, sea ice algae or diagenesis seem unable to explain the  
505 full range of variability seen in the FA δ<sup>13</sup>C record, the most plausible driver appears to be changes in surface  
506 water primary productivity. Coastal polynya environments in the Antarctic are areas of very high primary  
507 productivity (Arrigo and van Dijken, 2003). The DTGC2011 core site sits near to the Dumont D'Urville  
508 polynya, and is just downstream of the larger and more productive MGP (Arrigo and van Dijken, 2003). In large  
509 polynyas such as the Ross Sea, primary productivity leads to intense drawdown of CO<sub>2</sub> in the surface waters,  
510 resulting in reduced fractionation by the phytoplankton during photosynthesis (Villinski et al., 2008). In the  
511 Ross Sea, surface water CO<sub>2</sub> has been observed to drop to below 100 ppm during times of large phytoplankton  
512 blooms (Tortell et al., 2011) demonstrating that primary productivity can play a key role in controlling surface  
513 water CO<sub>2</sub> concentrations in a productive polynya environment. Arrigo et al. (2015) found the MGP to be the 8<sup>th</sup>  
514 most productive polynya in the Antarctic (out of 46) based on total net primary productivity during their  
515 sampling period, and Shadwick et al. (2014) observed CO<sub>2</sub> drawdown in the MGP during the summer months.

516 Therefore, we suggest that FA δ<sup>13</sup>C signals recorded in DTGC2011 is predominantly a signal of surface water  
517 CO<sub>2</sub> driven by primary productivity. Indeed, the potential for the δ<sup>13</sup>C of sedimentary lipids to track surface  
518 water primary productivity has been recognised in the highly productive Ross Sea polynya. High variability in  
519 surface water CO<sub>2</sub> values have been measured across the polynya during the summer months (December –  
520 January), ranging from less than 150 ppm in the western Ross Sea near the coast, to >400 ppm on the northern  
521 edge of the polynya. This pattern was closely correlated with diatom abundances, indicating intense drawdown  
522 of CO<sub>2</sub> in the western region where diatom abundances were highest (Tortell et al., 2011). This spatial variation  
523 in productivity is recorded in particulate organic carbon (POC) δ<sup>13</sup>C, and is also tracked in the surface sediments  
524 by total organic carbon (TOC) δ<sup>13</sup>C and algal sterol δ<sup>13</sup>C, all of which show significantly higher values in the  
525 western Ross Sea. This spatial pattern in sterol δ<sup>13</sup>C was concluded to be directly related to CO<sub>2</sub> drawdown at  
526 the surface, resulting in average sterol δ<sup>13</sup>C values varying from -27.9‰ in the west, where productivity is  
527 greatest, down to -33.5‰ further offshore (Villinski et al., 2008).

528 A similar relationship is evident in Prydz Bay, where POC  $\delta^{13}\text{C}$  was found to be positively correlated with POC  
529 concentration and negatively correlated with nutrient concentration, indicating greater drawdown of  $\text{CO}_2$  and  
530 nutrients under high productivity levels (Zhang et al., 2014).

531 This suggests it is possible to apply FA  $\delta^{13}\text{C}$  as a palaeoproductivity indicator in the highly productive Adélie  
532 polynya environment. However, it is important to constrain the most likely season and habitat being represented,  
533 since phytoplankton assemblages vary both spatially (e.g. ice edge or open water) and temporally (e.g. spring or  
534 summer). The increase in high sedimentation rate ( $1\text{-}2\text{ cm yr}^{-1}$ ) within the Adélie Basin is thought to result, on  
535 top of regional high productivity, from syndepositional focusing processes bringing biogenic debris from the  
536 shallower Adélie and Mertz banks to the ca. 1,000 m deep basin (Escutia et al., 2011). Thus, it is likely that core  
537 DTGC2011 contains material from a wide area, including both the Mertz and Dumont d'Urville polynyas, and  
538 areas both near the coast and further offshore, meaning it is quite possible that the  $\text{C}_{18}$  and  $\text{C}_{24}$  FAs are  
539 integrating palaeoproductivity changes weighted towards different regional environments, which would explain  
540 their different trends. Furthermore, surface water  $\text{CO}_2$  can vary spatially, such as in the Ross Sea polynya where  
541 Tortell et al. (2011) measured surface water  $\text{CO}_2$  values ranging between 100 and 400 ppm. Thus, it is likely  
542 that these two areas offshore Adélie Land where the  $\text{C}_{18}$  and  $\text{C}_{24}$  FAs are being produced will also have differing  
543 surface water  $\text{CO}_2$  concentrations and trends.

#### 544 4.3 Comparison of fatty acid $\delta^{13}\text{C}$ with other proxy data

545 Comparison of down-core variations in FA  $\delta^{13}\text{C}$  with other proxy data can also be used to decipher the main  
546 signal recorded. Comparison between  $\delta^{13}\text{C}_{24\text{FA}}$  and the major diatom species abundances within the core  
547 (*Fragilariopsis kerguelensis*, *Fragilariopsis curta*, *Fragilariopsis rhombica*, *Fragilariopsis cylindrus*,  
548 *Chaetoceros* resting spores) shows a reasonably close coherence with *Fragilariopsis kerguelensis*, particularly  
549 since ~1800 C.E. (Fig. 7). *Fragilariopsis kerguelensis* is an open water diatom species and one of the most  
550 dominant phytoplankton species offshore Adélie Land (Chiba et al., 2000), reaching its peak abundance in the  
551 summer (Crosta et al., 2007). This suggests that the  $\text{C}_{24}$  FA is being produced during the summer months and, as  
552 such, is reflecting productivity in more open waters. The  $\delta^{13}\text{C}_{24\text{FA}}$  record does not show any similarity to the sea-  
553 ice records, as inferred by HBI diene concentrations and abundances of *Fragilariopsis curta* (Fig. 6 and 7), here  
554 again suggesting that these compounds are being produced in open water during the summer months after sea  
555 ice has retreated.

556 As discussed above, *P. antarctica* is a likely producer for the  $\text{C}_{18}$  FA, a prymnesiophyte algae which has been  
557 observed in the Adélie region in summer months residing predominantly along the margin of fast ice, but also  
558 further offshore (Riaux-Gobin et al., 2013, 2011; Vaillancourt et al., 2003). The aversion of *F. kerguelensis* to  
559 sea ice (and thus also the  $\text{C}_{24}$  FA producer) in contrast to *P. antarctica*, may explain the clear lack of coherence  
560 in the down-core trends in  $\delta^{13}\text{C}_{18\text{FA}}$  and  $\delta^{13}\text{C}_{24\text{FA}}$  (Fig. 7). Thus, we hypothesise that  $\delta^{13}\text{C}_{18\text{FA}}$  is recording surface  
561 water  $\text{CO}_2$  driven by productivity in the MIZ, whilst  $\delta^{13}\text{C}_{24\text{FA}}$  is recording surface water  $\text{CO}_2$  in more open  
562 water, further from the sea-ice edge.

563 HBI diene concentrations indicate elevated fast ice cover between ~1919 and 1970 C.E., with a particular peak  
564 between 1942 and 1970 C.E., after which concentrations rapidly decline and remain low until the top of the core  
565 (Fig. 7). Abundances of *F. curta*, used as a sea-ice proxy, similarly show peaks at this time indicate increased

566 sea-ice concentration (Campagne, 2015) (Fig. 7).  $\delta^{13}\text{C}_{18\text{FA}}$  indicates a period of low productivity between ~1922  
567 and 1977 C.E., broadly overlapping with this period of elevated fast ice concentration (Fig. 7), with a mean  
568 value of -27.12‰. This is compared to the mean value of -26.23‰ in the subsequent period (~1978 to 1998  
569 C.E.) during which HBI diene concentration remain low (Fig. 7). This suggests that productivity in the coastal  
570 region was reduced, while sea-ice concentrations were high. This might be expected during a period of  
571 enhanced ice cover – perhaps representing a reduction in the amount of open water, or a shorter open water  
572 season – since the majority of productivity generally takes place within open water (Wilson et al., 1986).

573 Furthermore,  $\delta^{13}\text{C}_{18\text{FA}}$  shows a broad similarity with *Chaetoceros* resting spores (CRS) on a centennial scale,  
574 with lower productivity at the start of the record, ca. 1587 to 1662 C.E., followed by an increase in both proxies  
575 in the middle part of the record, where  $\delta^{13}\text{C}_{18\text{FA}}$  becomes relatively stable and CRS reaches its highest  
576 abundances of the record. This is then followed in the latter part of the record, after ca. 1900 C.E., by both  
577 proxies displaying lower values overall. CRS are associated with high nutrient levels and surface water  
578 stratification along the edge of receding sea ice, often following high productivity events (Crosta et al., 2008).  
579 The broad similarity to CRS, with lower values recorded during periods of high sea-ice concentrations, suggests  
580 that  $\delta^{13}\text{C}_{18\text{FA}}$  is similarly responding to productivity in stratified water at the ice edge. This supports the  
581 hypothesis that  $\delta^{13}\text{C}_{18\text{FA}}$  is recording primary productivity in the MIZ. Little similarity is evident between the  
582 fatty acid isotope records and *F. cylindrus* and *F. rhombica*.

## 583 5 Conclusions

584 FAs identified within core DTGC2011, recovered from offshore Adélie Land, were analysed for their  
585 concentrations and carbon isotope compositions to assess their utility as a palaeoproductivity proxy in an  
586 Antarctic polynya environment. The  $\text{C}_{18}$  and  $\text{C}_{24}$  compounds yielded the best isotope measurements and show  
587 very different  $\delta^{13}\text{C}$  trends, suggesting they are being produced by different species in different habitats and/or  
588 seasons. here Although we have made parsimonious interpretations, there are clearly uncertainties in interpreting  
589 the FA  $\delta^{13}\text{C}$ , as various assumptions have been made. The producers of the  $\text{C}_{18}$  and especially the  $\text{C}_{24}$  FAs is  
590 a key source of uncertainty and will require further work to further elucidate. The possibility of inputs of FAs  
591 from multiple sources, in particular from organisms further up the food chain, has consequences for their  
592 interpretation since this could mean the  $\delta^{13}\text{C}$  FA is not fully reflecting just surface water conditions. Other key  
593 uncertainties are the magnitude of upwelling of  $\text{CO}_2$  at the site in comparison to drawdown by phytoplankton,  
594 and the potential role of changes in air-sea  $\text{CO}_2$  exchange.

595 Despite this, we argue that FA  $\delta^{13}\text{C}$  has the potential to be used as a productivity proxy, but would be best used  
596 in parallel with other environmental proxies such as diatoms abundances or HBIs. Comparison with other proxy  
597 data and information from previous studies suggests that the  $\text{C}_{18}$  compound may be predominantly produced by  
598 *P. antarctica*, with  $\delta^{13}\text{C}_{18\text{FA}}$  reflecting productivity changes in the marginal ice zone, where it is sensitive to  
599 changes in ice cover. In contrast,  $\delta^{13}\text{C}_{24\text{FA}}$ , which compares well with abundances of the open water diatom *F*  
600 *kerguelensis* may be reflecting summer productivity further offshore, in open waters where it is less sensitive to  
601 fast ice changes. The use of  $\delta^{13}\text{C}$  analysis of multiple FA compounds, opposed to individual compounds or  
602 bulk isotope analysis, allows a more detailed insight into the palaeoproductivity dynamics of the region, with the  
603 potential to separate productivity trends within different habitats.



604

605 **References**

- 606 Anderson, R.F., Ali, S., Bradtmiller, L.I., et al. (2009) Wind-driven upwelling in the Southern Ocean and the  
607 deglacial rise in atmospheric CO<sub>2</sub>. *Science (New York, N.Y.)*, 323 (5920): 1443–1448.  
608 doi:10.1126/science.1167441.
- 609 Archambeau, A.S., Pierre, C., Poisson, A., et al. (1998) Distributions of oxygen and carbon stable isotopes and  
610 CFC-12 in the water masses of the Southern Ocean at 30°E from South Africa to Antarctica: Results of the  
611 CIVI1 cruise. *Journal of Marine Systems*, 17 (1–4): 25–38. doi:10.1016/S0924-7963(98)00027-X.
- 612 Arrigo, K. R. (2007) ‘Chapter 7 Physical Control of Primary Productivity in Arctic and Antarctic Polynyas’,  
613 Elsevier Oceanography Series, 74(06), pp. 223–238. doi: 10.1016/S0422-9894(06)74007-7. Arrigo, K.R., van  
614 Dijken, G. and Long, M. (2008) Coastal Southern Ocean: A strong anthropogenic CO<sub>2</sub> sink. *Geophysical*  
615 *Research Letters*, 35 (21): 1–6. doi:10.1029/2008GL035624.
- 616 Arrigo, K.R. and van Dijken, G.L. (2003) Phytoplankton dynamics within 37 Antarctic coastal polynya systems.  
617 *Journal of Geophysical Research*, 108 (C8): 3271. doi:10.1029/2002JC001739.
- 618 Arrigo, K.R., van Dijken, G.L. and Strong, A.L. (2015) Environmental controls of marine productivity hot spots  
619 around Antarctica. *Journal of Geophysical Research: Oceans*, pp. 2121–2128. doi:10.1002/jgrc.20224.
- 620 Arrigo, K.R., Robinson, D.H., Worthen, D.L., et al. (1999) Community Phytoplankton Structure and the  
621 Drawdown of and CO<sub>2</sub> in the Nutrients Southern Ocean. *Science*, 283 (5400): 365–367.
- 622 Ashley, K. E., Bendle, J. A., McKay, R., Etourneau, J., Jimenez-Espejo, F. J., Condrón, A., Albot, A., Crosta,  
623 X., Riesselman, C., Seki, O., Massé, G., Golledge, N. R., Gasson, E., Lowry, D. P., Barrand, N. E., Johnson, K.,  
624 Bertler, N., Escutia, C., and Dunbar, R.: Mid-Holocene Antarctic sea-ice increase driven by marine ice sheet  
625 retreat, *Clim. Past Discuss.*, <https://doi.org/10.5194/cp-2020-3>, in review, 2020.
- 626 Belt, S.T., Allard, W.G., Rintatalo, J., et al. (2000) Clay and acid catalysed isomerisation and cyclisation  
627 reactions of highly branched isoprenoid (HBI) alkenes: Implications for sedimentary reactions and distributions.  
628 *Geochimica et Cosmochimica Acta*, 64 (19): 3337–3345. doi:10.1016/S0016-7037(00)00444-0.
- 629 Belt, S.T., Brown, T.A., Smik, L., et al. (2017) Identification of C<sub>25</sub> highly branched isoprenoid (HBI) alkenes  
630 in diatoms of the genus *Rhizosolenia* in polar and sub-polar marine phytoplankton. *Organic Geochemistry*, 110:  
631 65–72. doi:10.1016/j.orggeochem.2017.05.007.
- 632 Belt, S.T. and Müller, J. (2013) The Arctic sea ice biomarker IP 25 : a review of current understanding ,  
633 recommendations for future research and applications in palaeo sea ice reconstructions. *Quaternary Science*  
634 *Reviews*, 79: 9–25. doi:10.1016/j.quascirev.2012.12.001.
- 635 Belt, S.T., Smik, L., Brown, T.A., et al. (2016) Source identification and distribution reveals the potential of the  
636 geochemical Antarctic sea ice proxy IPSO<sub>25</sub>. *Nature Communications*, 7: 1–10. doi:10.1038/ncomms12655.
- 637 Beucher, C., Tre, P., Hapette, A., et al. (2004) Intense summer Si-recycling in the surface Southern Ocean., 31:

638 0–3. doi:10.1029/2003GL018998.

639 Budge, S.M., Wooller, M.J., Springer, A.M., et al. (2008) Tracing carbon flow in an arctic marine food web  
640 using fatty acid-stable isotope analysis. *Oecologia*, 157 (1): 117–129. doi:10.1007/s00442-008-1053-7.

641 Burke, A. and Robinson, L.F. (2012) The Southern Ocean’s Role in Carbon Exchange During the Last  
642 Deglaciation. *Science*, 335: 557–561.

643 Cabedo Sanz, P., Smik, L. and Belt, S.T. (2016) On the stability of various highly branched isoprenoid (HBI)  
644 lipids in stored sediments and sediment extracts. *Organic Geochemistry*, 97: 74–77.  
645 doi:10.1016/j.orggeochem.2016.04.010.

646 Campagne, P. (2015) *Étude de la variabilité des conditions océanographiques et climatiques en Antarctique de*  
647 *l’Est (Terre Adélie-Georges V) au cours de l’Holocène tardif et de la période instrumentale*. L’Université de  
648 Bordeaux.

649 Ceccaroni, L., Frank, M., Frignani, M., Langone, L., Ravaoli, M. & Mangini, A. 1998. Late Quaternary  
650 fluctuations of biogenic component fluxes on the continental slope of the Ross Sea, Antarctica. *Journal of*  
651 *Marine Systems*, 17, 515–525.

652 Chiba, S., Hirawake, T., Ushio, S., et al. (2000) An overview of the biological/oceanographic survey by the  
653 RTV Umitaka-Maru III off Adelie Land, Antarctica in January-February 1996. *Deep-Sea Research Part II:*  
654 *Topical Studies in Oceanography*, 47 (12–13): 2589–2613. doi:10.1016/S0967-0645(00)00037-0.

655 Colombo, J.C., Silverberg, N. and Gearing, J.N. (1997) Lipid biogeochemistry in the Laurentian Trough--II.  
656 Changes in composition of fatty acids, sterols and aliphatic hydrocarbons during early diagenesis. *Org.*  
657 *Geochem.*, 26 (3): 257–274.

658 Crosta, X., Crespin, J., Billy, I., et al. (2005) Major factors controlling Holocene d13Corg changes in a seasonal  
659 sea-ice environment, Adelie Land, East Antarctica. *Global Biogeochemical Cycles*, 19 (4).  
660 doi:10.1029/2004GB002426.

661 Crosta, X., Debret, M., Denis, D., et al. (2007) Holocene long- and short-term climate changes off Adelie Land,  
662 East Antarctica. *Geochemistry Geophysics Geosystems*, 8 (11): n/a-n/a. doi:10.1029/2007GC001718.

663 Crosta X, Shukla S.K., Ther O., Ikehara M., Yamane M., Yokoyama Y. (2020) Last Abundant Appearance  
664 Datum of Hemidiscus karstenii driven by climate change. *Marine Micropaleontology*,  
665 doi:10.1016/j.marmicro.2020.101861.

666 Dalsgaard, J., St. John, M., Kattner, G., et al. (2003) Fatty acid trophic markers in the pelagic marine  
667 environment. *Advances in Marine Biology*. 46 pp. 225–340. doi:10.1016/S0065-2881(03)46005-7.

668 DiTullio, G.R., Grebmeier, J.M., Arrigo, K.R., et al. (2000) Rapid and early export of Phaeocystis antarctica  
669 blooms in the Ross Sea, Antarctica. *Nature*, 404 (6778): 595–598. doi:10.1038/35007061.

670 Escutia, C., Brinkhuis, H., Klaus, A., et al. (2011) *Expedition 318 summary*.  
671 doi:10.2204/iodp.proc.318.101.2011.

672 Farquhar, G.D., O’Leary, M.H. and Berry, J.A. (1982) On the Relationship between Carbon Isotope  
673 Discrimination and the Intercellular Carbon dioxide Concentration in Leaves. *Australian Journal of Plant*  
674 *Physiology*, 9: 121–137.

675 Fischer, G., Schneider, R., Müller, P.J., et al. (1997) Anthropogenic CO<sub>2</sub> in Southern Ocean surface waters:  
676 Evidence from stable organic carbon isotopes. *Terra Nova*, 9 (4): 153–157. doi:10.1046/j.1365-3121.1997.d01-  
677 29.x.

678 Francey, R.J., Allison, C.E., Etheridge, D.M., et al. (1999) A 1000-year high precision record of  $\delta^{13}\text{C}$  in  
679 atmospheric CO<sub>2</sub>. *Tellus, Series B: Chemical and Physical Meteorology*, 51 (2): 170–193.

680 Frignani, M., Giglio, F., Langone, L., Ravaioli, M. & Mangini, A. 1998. Late Pleistocene- Holocene  
681 sedimentary fluxes of organic carbon and biogenic silica in the northwestern Ross Sea, Antarctica. *Annals of*  
682 *Glaciology*, **27**, 697–703.

683

684 Gibson, J.A.E., Trull, T., Nichols, P.D., et al. (1999) Sedimentation of <sup>13</sup>C-rich organic matter from Antarctic  
685 sea-ice algae: A potential indicator of past sea-ice extent. *Geology*, 27 (4): 331–334. doi:10.1130/0091-  
686 7613(1999)027<0331:SOCROM>2.3.CO;2.

687 Gilchrist, H. (2018) *A high-resolution record of sea ice, glacial and biological dynamics from an Antarctic*  
688 *coast environment*. University of Birmingham.

689 Haddad, R.I., Martens, C.S. and Farrington, J.W. (1992) Quantifying early diagenesis of fatty acids in a rapidly  
690 accumulating coastal marine sediment. *Organic Geochemistry*, 19 (1–3): 205–216. doi:10.1016/0146-  
691 6380(92)90037-X.

692 Henley, S.F., Annett, A.L., Ganeshram, R.S., et al. (2012) Factors influencing the stable carbon isotopic  
693 composition of suspended and sinking organic matter in the coastal Antarctic sea ice environment.  
694 *Biogeosciences*, 9 (3): 1137–1157. doi:10.5194/bg-9-1137-2012.

695 Johns, L. et al. (1999) ‘Identification of a C<sub>25</sub> highly branched isoprenoid (HBI) diene in Antarctic sediments,  
696 Antarctic sea-ice diatoms and cultured diatoms’, *Organic Geochemistry*, 30(11), pp. 1471–1475. doi:  
697 10.1016/S0146-6380(99)00112-6.

698 Keeling, C.D., Piper, S.C., Bacastow, R.B., et al. (2005) “Atmospheric CO<sub>2</sub> and <sup>13</sup>CO<sub>2</sub> Exchange with the  
699 Terrestrial Biosphere and Oceans from 1978 to 2000: Observations and Carbon Cycle Implications.” In A  
700 History of Atmospheric CO<sub>2</sub> and Its Effects on Plants, Animals, and Ecosystems. doi:10.1007/0-387-27048-  
701 5\_5.

702 Kocczynska, E.E., Goeyens, L., Semeneh, M., et al. (1995) Phytoplankton Composition and Cell Carbon  
703 Distribution in Prydz Bay, Antarctica - Relation To Organic Particulate Matter and Its Delta-C-13 Values.  
704 *Journal of Plankton Research*, 17 (4): 685–707. doi:10.1093/plankt/17.4.685.

705 Leblond, J.D. and Chapman, P.J. (2000) LIPID CLASS DISTRIBUTION OF HIGHLY UNSATURATED  
706 LONG CHAIN FATTY ACIDS IN MARINE DINOFLAGELLATES. *Journal of Phycology*, 36: 1103–1108.

707 MacFarling Meure, C., Etheridge, D., Trudinger, C., et al. (2006) Law Dome CO<sub>2</sub>, CH<sub>4</sub> and N<sub>2</sub>O ice core  
708 records extended to 2000 years BP. *Geophysical Research Letters*, 33 (14): 1–4. doi:10.1029/2006GL026152.

709 Mackensen, A. (2001) Oxygen and carbon stable isotope tracers of Weddell sea water masses: New data and  
710 some paleoceanographic implications. *Deep-Sea Research Part I: Oceanographic Research Papers*, 48 (6):  
711 1401–1422. doi:10.1016/S0967-0637(00)00093-5.

712 Massé, G., Belt, S.T., Crosta, X., et al. (2011) Highly branched isoprenoids as proxies for variable sea ice  
713 conditions in the Southern Ocean. *Antarctic Science*, 23 (5): 487–498. doi:10.1017/S0954102011000381.

714 Matsuda, H. (1978) Early diagenesis of fatty acids in lacustrine sediments-III. Changes in fatty acid composition  
715 in the sediments from a brackish water lake. *Geochimica et Cosmochimica Acta*, 42: 1027–1034.

716 Matsuda, H. and Koyama, T. (1977) Early diagenesis of fatty acids in lacustrine sediments-I. Identification and  
717 distribution of fatty acids in recent sediment from a freshwater lake. *Geochimica et Cosmochimica Acta*, 41 (6):  
718 777–783. doi:10.1016/0016-7037(77)90048-5.

719 Moisan, T.A. and Mitchell, B.G. (1999) Photophysiological acclimation of *Phaeocystis antarctica* Karsten under  
720 light limitation. *Limnology and Oceanography*, 44 (2): 247–258. doi:10.4319/lo.1999.44.2.0247.

721 Pancost, R.D. and Boot, C.S. (2004) The palaeoclimatic utility of terrestrial biomarkers in marine sediments.  
722 *Marine Chemistry*, 92 (1–4 SPEC. ISS.): 239–261. doi:10.1016/j.marchem.2004.06.029.

723 Popp, B. N. et al. (1999) ‘Controls on the carbon isotopic composition of Southern Ocean phytoplankton’,  
724 *Global Biogeochemical Cycles*, 13(4), pp. 827–843. doi: 10.1029/1999GB900041.

725 Poulton, A.J., Mark Moore, C., Seeyave, S., et al. (2007) Phytoplankton community composition around the  
726 Crozet Plateau, with emphasis on diatoms and *Phaeocystis*. *Deep-Sea Research Part II: Topical Studies in*  
727 *Oceanography*, 54 (18–20): 2085–2105. doi:10.1016/j.dsr2.2007.06.005.

728 Rau, G.H., Takahashi, T. and Des Marais, D.J. (1989) Latitudinal variations in plankton  $\delta^{13}\text{C}$ : Implications for  
729 CO<sub>2</sub> and productivity in past oceans. *Nature*, 341 (6242): 516–518.

730 Riaux-gobin, C., Dieckmann, G.S., Poulin, M., et al. (2013) *Environmental conditions , particle flux and*  
731 *sympagic microalgal succession in spring before the sea-ice break-up in Adélie Land , East Antarctica*  
732 *Environmental conditions , particle flux and sympagic microalgal ´ lie Land , succession in spring before t.,*  
733 (May 2014): 0–25. doi:10.3402/polar.v32i0.19675.

734 Riaux-Gobin, C., Dieckmann, G.S., Poulin, M., et al. (2013) Environmental conditions, particle flux and  
735 sympagic microalgal succession in spring before the sea-ice break-up in Adélie Land, East Antarctica. *Polar*  
736 *Research*, 32 (SUPPL.): 0–25. doi:10.3402/polar.v32i0.19675.

737 Riaux-Gobin, C., Poulin, M., Dieckmann, G., et al. (2011) Spring phytoplankton onset after the ice break-up and  
738 sea-ice signature (Adélie Land, East Antarctica). *Polar Research*, 30 (SUPPL.1).  
739 doi:10.3402/polar.v30i0.5910.

740 Roden, N.P., Shadwick, E.H., Tilbrook, B., et al. (2013) Annual cycle of carbonate chemistry and decadal

741 change in coastal Prydz Bay, East Antarctica. *Marine Chemistry*, 155: 135–147.  
742 doi:10.1016/j.marchem.2013.06.006.

743 Salminen, T.A., Eklund, D.M., Joly, V., et al. (2018) Deciphering the evolution and development of the cuticle  
744 by studying lipid transfer proteins in mosses and liverworts. *Plants*, 7 (1). doi:10.3390/plants7010006.

745 Sambrotto, R.N., Matsuda, A., Vaillancourt, R., et al. (2003) Summer plankton production and nutrient  
746 consumption patterns in the Mertz Glacier Region of East Antarctica. *Deep-Sea Research Part II: Topical  
747 Studies in Oceanography*, 50 (8–9): 1393–1414. doi:10.1016/S0967-0645(03)00076-6.

748 Shadwick, E.H., Tilbrook, B. and Williams, G.D. (2014) Carbonate chemistry in the Mertz Polynya (East  
749 Antarctica): Biological and physical modification of dense water outflows and the export of anthropogenic CO<sub>2</sub>.  
750 *Journal of Geophysical Research: Oceans*, 119 (1): 1–14. doi:10.1002/2013JC009286.

751 Shevenell, A.E. and Kennett, J.P. (2002) *Antarctic Holocene climate change : A benthic foraminiferal stable  
752 isotope record from Palmer Deep.*, 17 (2).

753 Sigman, D. and Boyle, E. (2000) Glacial/interglacial variations in atmospheric carbon dioxide. *Nature*, 407  
754 (6806): 859–869.

755 Sinninghe Damsté, J.S., Rijpstra, W.I.C., Coolen, M.J.L., et al. (2007) Rapid sulfurisation of highly branched  
756 isoprenoid (HBI) alkenes in sulfidic Holocene sediments from Ellis Fjord, Antarctica. *Organic Geochemistry*,  
757 38 (1): 128–139. doi:10.1016/j.orggeochem.2006.08.003.

758 Skerratt, J.H., Davidson, A.D., Nichols, P.D., et al. (1998) Effect of UV-B on lipid content of three antarctic  
759 marine phytoplankton. *Phytochemistry*, 49 (4): 999–1007. doi:10.1016/S0031-9422(97)01068-6.

760 Smik, L., Belt, S.T., Lieser, J.L., et al. (2016) Distributions of highly branched isoprenoid alkenes and other  
761 algal lipids in surface waters from East Antarctica: Further insights for biomarker-based paleo sea-ice  
762 reconstruction. *Organic Geochemistry*, 95: 71–80. doi:10.1016/j.orggeochem.2016.02.011.

763 Sun, M.Y., Zou, L., Dai, J., et al. (2004) Molecular carbon isotopic fractionation of algal lipids during  
764 decomposition in natural oxic and anoxic seawaters. *Organic Geochemistry*, 35 (8): 895–908.  
765 doi:10.1016/j.orggeochem.2004.04.001.

766 Sweeney, C. (2003) “The annual cycle of surface water CO<sub>2</sub> And O<sub>2</sub> in the Ross Sea: A model for gas  
767 exchange on the continental shelves of Antarctica.” *In Antarctic Research Series Vol 78*. doi:10.1029/078ars19.

768 Takahashi, T., Sutherland, S.C., Wanninkhof, R., et al. (2009) Climatological mean and decadal change in  
769 surface ocean pCO<sub>2</sub>, and net sea-air CO<sub>2</sub> flux over the global oceans. *Deep-Sea Research Part II: Topical  
770 Studies in Oceanography*, 56 (8–10): 554–577. doi:10.1016/j.dsr2.2008.12.009.

771 Tortell, P.D., Guéguen, C., Long, M.C., et al. (2011) Spatial variability and temporal dynamics of surface water  
772 pCO<sub>2</sub>, δO<sub>2</sub>/Ar and dimethylsulfide in the Ross Sea, Antarctica. *Deep-Sea Research Part I: Oceanographic  
773 Research Papers*, 58 (3): 241–259. doi:10.1016/j.dsr.2010.12.006.

774 Tréguer, P., Bowler, C., Moriceau, B., et al. (2017) Influence of diatom diversity on the ocean biological carbon

775 pump. *Nature Geoscience*. doi:10.1038/s41561-017-0028-x.

776 Vaillancourt, R.D., Sambrotto, R.N., Green, S., et al. (2003) Phytoplankton biomass and photosynthetic  
777 competency in the summertime Mertz Glacier region of East Antarctica. *Deep-Sea Research Part II: Topical  
778 Studies in Oceanography*, 50 (8–9): 1415–1440. doi:10.1016/S0967-0645(03)00077-8.

779 Villinski, J.C., Hayes, J.M., Brassell, S.C., et al. (2008) Sedimentary sterols as biogeochemical indicators in the  
780 Southern Ocean. *Organic Geochemistry*, 39 (5): 567–588. doi:10.1016/j.orggeochem.2008.01.009.

781 Wakeham, S.G., Lee, C., Farrington, J.W., et al. (1984) Biogeochemistry of particulate organic matter in the  
782 oceans: results from sediment trap experiments. *Deep Sea Research Part A, Oceanographic Research Papers*,  
783 31 (5): 509–528. doi:10.1016/0198-0149(84)90099-2.

784 Williams, G.D. and Bindoff, N.L. (2003) Wintertime oceanography of the Adélie Depression. *Deep-Sea  
785 Research Part II: Topical Studies in Oceanography*, 50 (8–9): 1373–1392. doi:10.1016/S0967-0645(03)00074-  
786 2.

787 Wilson, D.L., Smith, W.O. and Nelson, David, M. (1986) *Phytoplankton bloom dynamics of the western Ross  
788 Sea ice edge - I. Primary productivity and species-specific production.*, 33 (10): 1375–1387.

789 Wong, W.W. and Sackett, W.M. (1978) Fractionation of stable carbon isotopes by marine phytoplankton.  
790 *Geochimica et Cosmochimica Acta*, 42 (12): 1809–1815. doi:10.1016/0016-7037(78)90236-3.

791 Zhang, R., Zheng, M., Chen, M., et al. (2014) An isotopic perspective on the correlation of surface ocean carbon  
792 dynamics and sea ice melting in Prydz Bay (Antarctica) during austral summer. *Deep-Sea Research Part I:  
793 Oceanographic Research Papers*, 83: 24–33. doi:10.1016/j.dsr.2013.08.006.

794

795

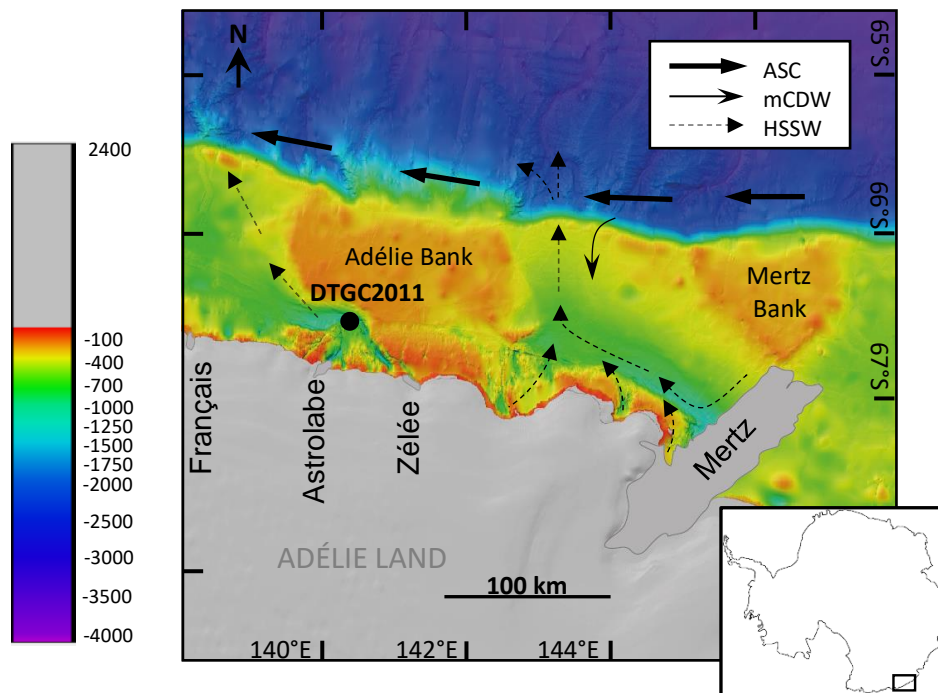


**Figure 1: Location of Site DTGC2011 on bathymetric map of the Adélie Land region (modified from Beaman et al., 2011), indicating positions of the main glaciers (prior to Mertz Glacier Tongue collapse in 2010) and pathways of the main water masses affecting the region: Antarctic Slope Current (ASC), Modified Circumpolar Deep Water (mCDW) and High Shelf Salinity Water (HSSW) (Williams and Bindoff, 2003).**

796

797

798

799

800

801

802

803

804

805

806

807

808

809

810  
811  
812  
813  
814  
815  
816  
817  
818  
819  
820  
821  
822  
823  
824  
825  
826  
827  
828  
829  
830  
831  
832  
833  
834

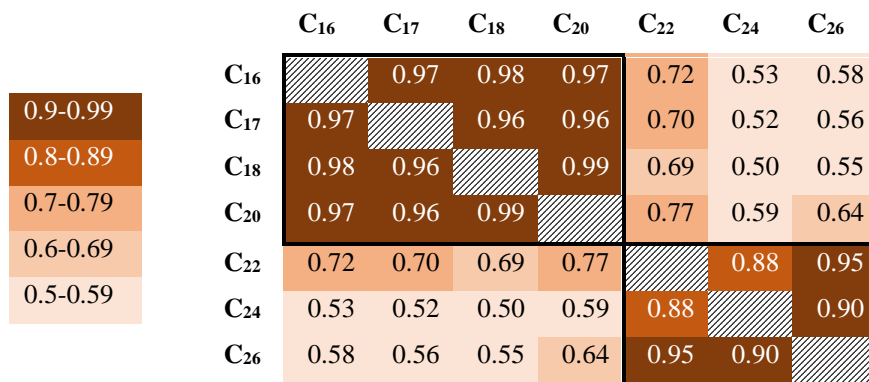


Figure 3: R<sup>2</sup> values for fatty acid concentrations throughout core DTGC2011. Values are colour coded according to the key on the left. Black border denotes correlations within each group.

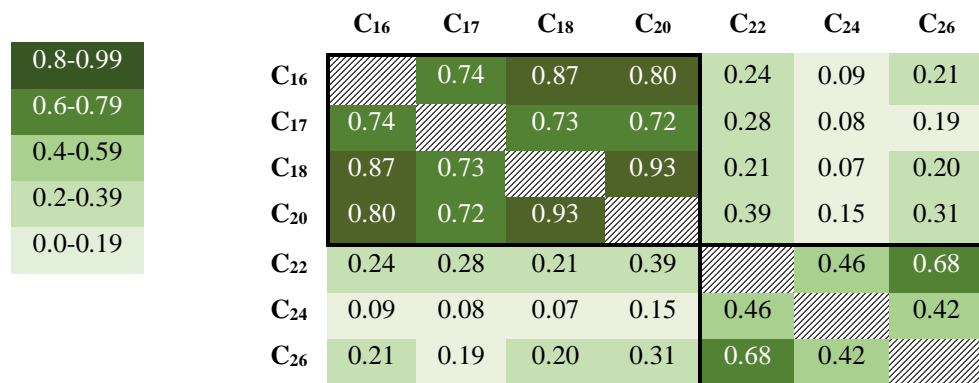


Figure 4: R<sup>2</sup> values for fatty acid concentrations in core DTGC2011 below 25 cm only. Values are colour coded according to the key on the left. Black border denotes correlations within each group.



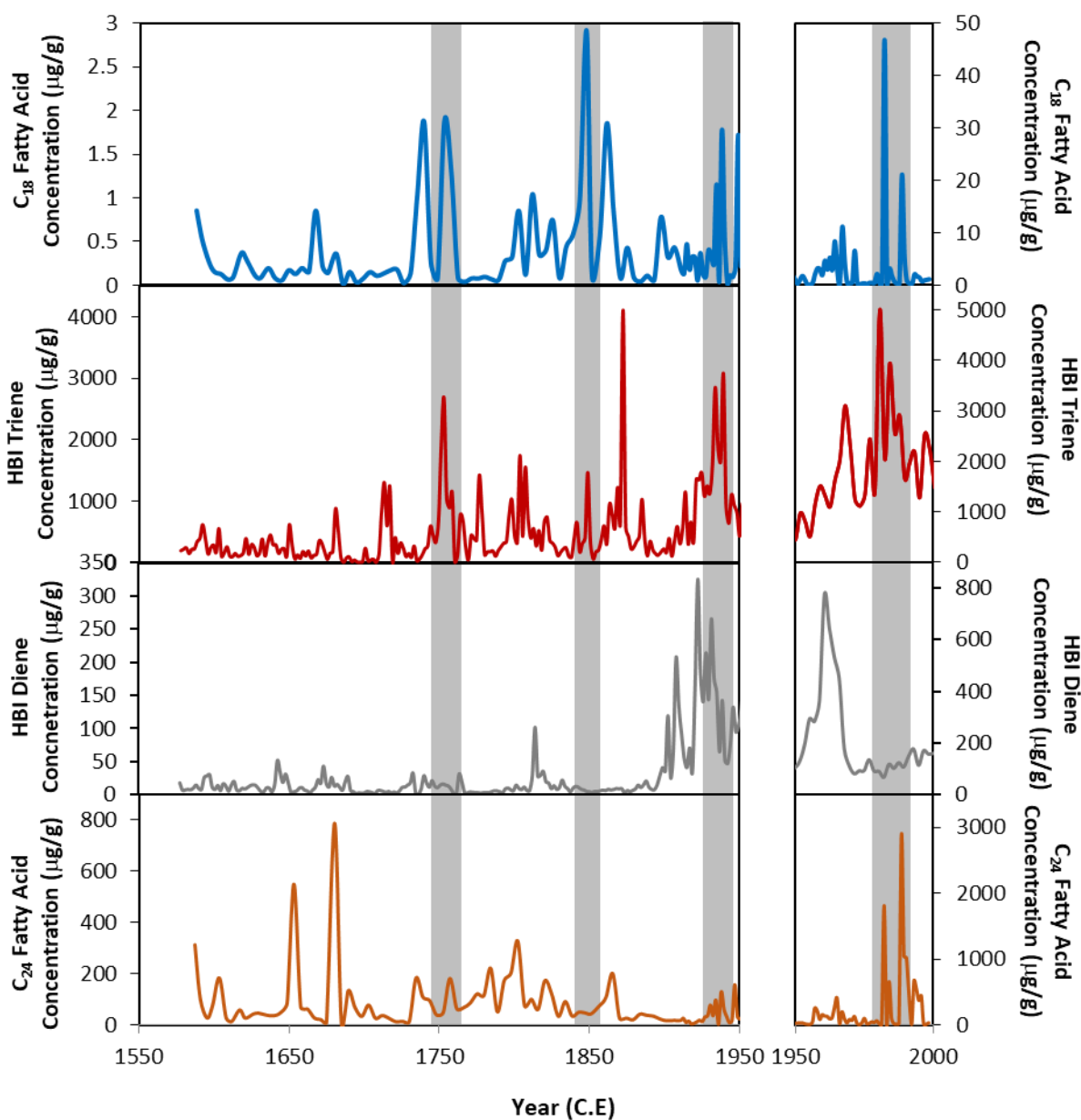
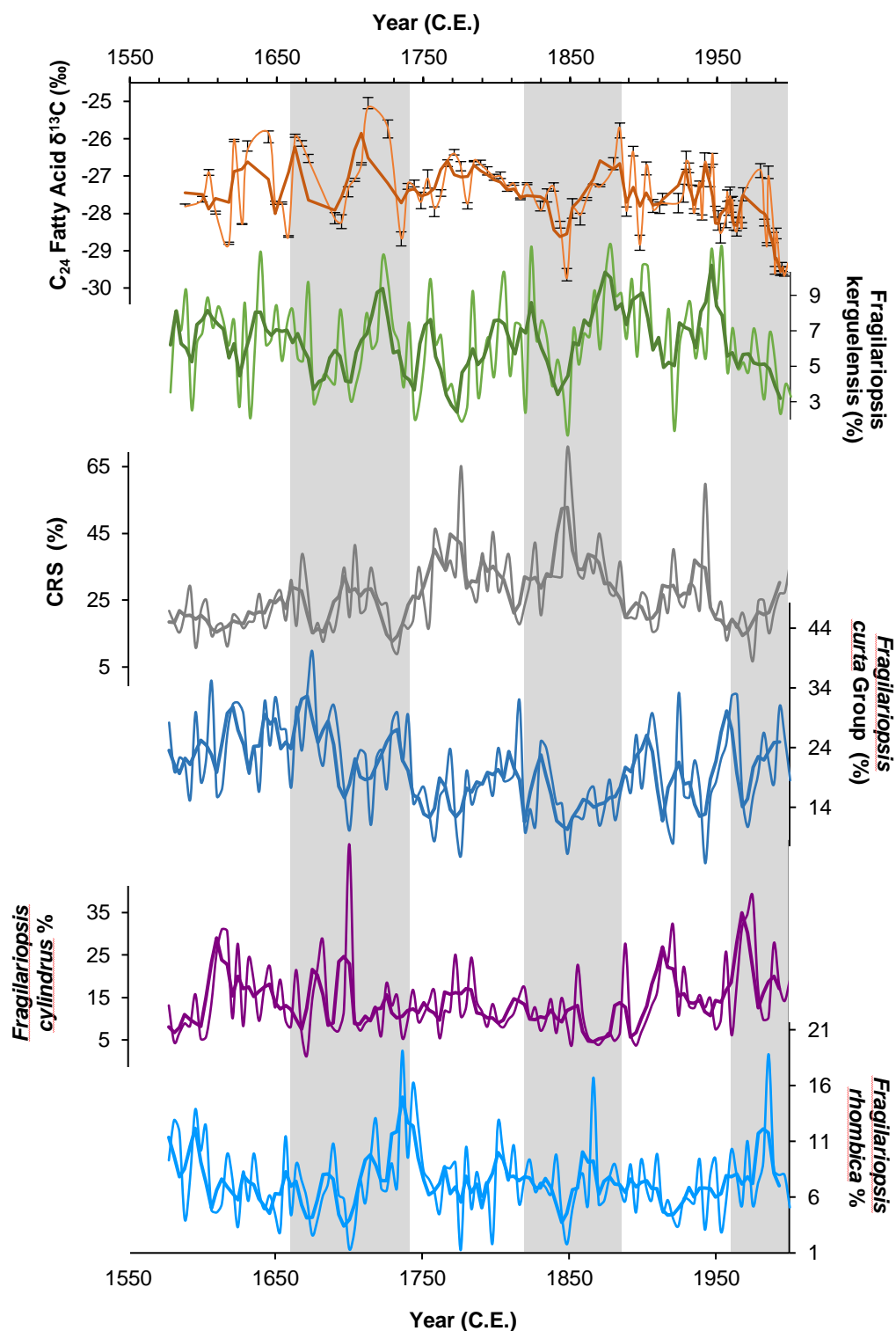
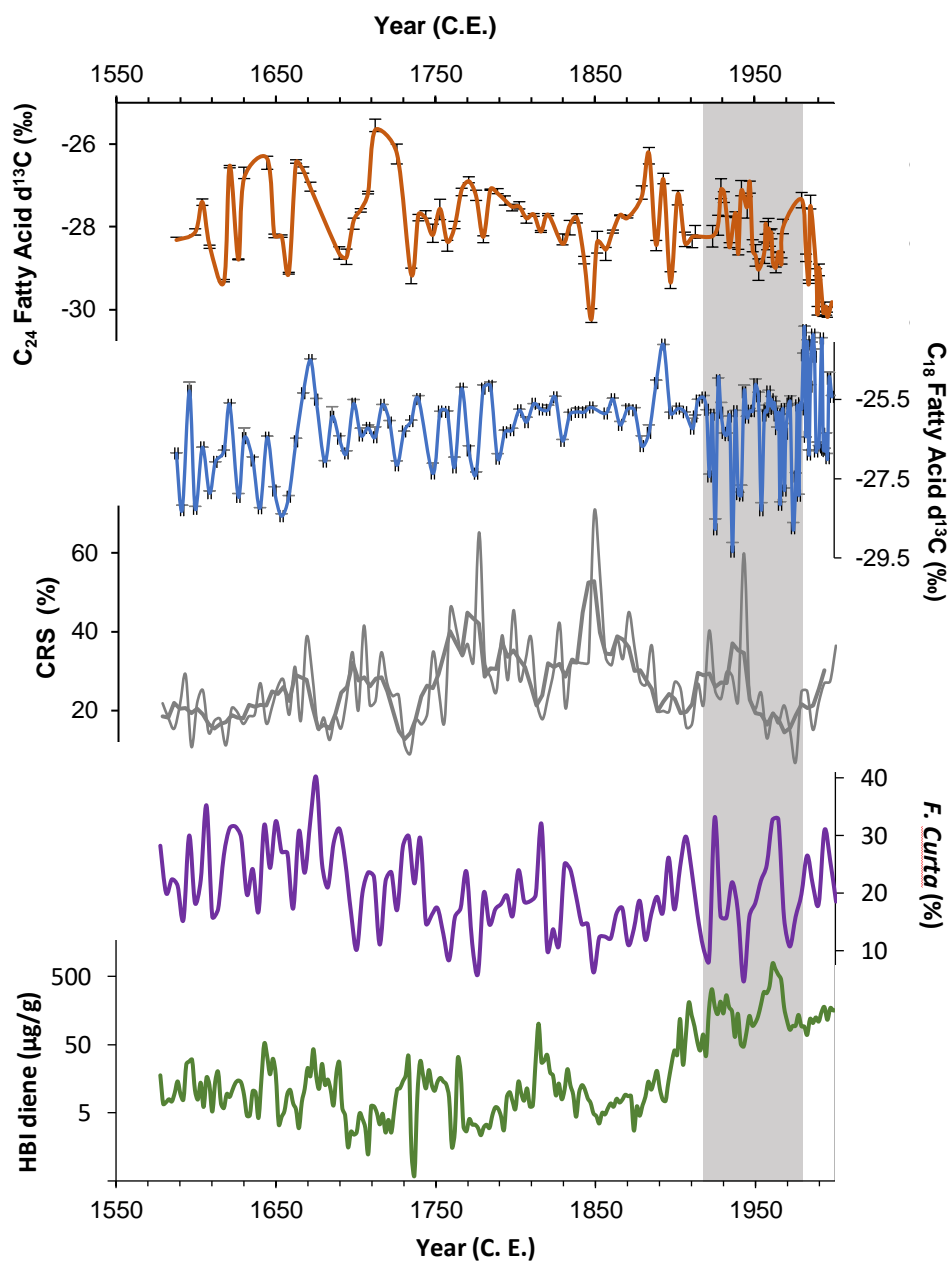


Figure 5: Concentrations of the  $\text{C}_{18}$  fatty acid (blue), the HBI triene (red), HBI diene (grey) (Campagne, 2015),  $\text{C}_{24}$  fatty acid (orange) from core DTGC2011. The left-hand panels show 1550 to 1950 C.E. and the right hand panels show 1950 to 2000 C.E., plotted on different y-axes due to the elevated concentrations in the top part of the core. Grey vertical bands highlight coincident peaks in  $\text{C}_{18}$  fatty acid and HBI triene records.



**Figure 6:**  $\delta^{13}\text{C}$  values of the  $\text{C}_{24}$  fatty acid (orange) and relative abundances (%) of the open water diatom *Fragilariopsis kerguelensis* (green). Also shown are relative abundances of the four most abundant diatom groups in DTGC2011. *Chaetoceros* resting spores (CRS; grey line), *Fragilariopsis curta* group (dark blue line), *Fragilariopsis cylindrus* (purple line) and *Fragilariopsis rhombica* (light blue line). Thick line represents 3-point moving average for each. Grey vertical bands highlight periods where  $\text{C}_{24}$  fatty acid  $\delta^{13}\text{C}$  is in phase with *F. kerguelensis*.



**Figure 7:**  $\delta^{13}\text{C}$  of the  $\text{C}_{24}$  (orange) and  $\text{C}_{18}$  (blue) fatty acid, HBI diene concentrations (green; plotted on a log scale) and relative abundances of *Fragilariopsis curta* plus *Fragilariopsis cylindrus* (purple). Latter two records reflect sea ice concentrations. Grey vertical band highlights period where low  $\text{C}_{18}$   $\delta^{13}\text{C}$  overlaps with elevated HBI diene concentrations.

839

840

841

842